A Study of Optoelectronic and Environmental Factors Affecting the Accuracy of Vehicle-Mounted Licence Plate Recognition

by

Martin Christian Rademeyer

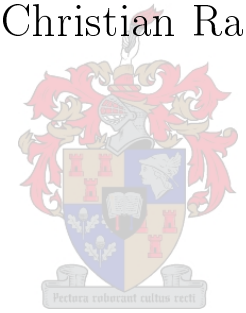

Thesis presented in partial fulfilment of the requirements for the degree of Master of Engineering (Electronic) in the Faculty of Engineering at Stellenbosch University

Study leaders: Prof. M.J. Booysen
Mr. A. Barnard

April 2019

Declaration

By submitting this report electronically, I declare that the entirety of the work contained therein is my own, original work, that I am the sole author thereof (save to the extent explicitly otherwise stated), that reproduction and publication thereof by Stellenbosch University will not infringe any third party rights and that I have not previously in its entirety or in part submitted it for obtaining any qualification.

Date: April 2019

Abstract

Across the world, licence plate recognition (LPR) technology has been used to combat vehicle-related crime in urban areas. However, commercially available LPR systems are expensive and not feasible for large scale adoption in developing countries. The development of a low-cost system will require an informed approach to selection of an appropriate camera, as well as a realistic understanding of the system's performance under various conditions.

This work investigated the effect of optoelectronic and environmental factors on the ability of vehicle-mounted LPR systems to correctly identify licence plates. A theoretical LPR camera model was developed to estimate the effect of different cameras, while the effects of motion, orientation and lighting were evaluated in a series of experimental tests.

The most influential optoelectronic factors were shown to be focus, focal length and image sensor resolution. Licence plates could theoretically be recognised across a large area using a fixed-focus prime lens mounted on a high-resolution image sensor. Furthermore, recognition was impaired during high-speed turn manoeuvres, as well as in cases where licence plates were orientated at more than a 45° angle to the camera. In night-time conditions, retroflective licence plates could be recognised at a distance comparable to that of daytime conditions, while oncoming headlights were shown to hinder accurate recognition.

The optoelectronic model proved useful for selection of a cost-effective camera for use in an open source LPR system. Moreover, the study of environmental factors provided valuable insight into the limitations of LPR systems in various environmental and traffic conditions.

Keywords: Automatic licence plate recognition (ALPR, LPR), automatic number plate recognition (ANPR), recognition accuracy, vehicle-mounted camera, urban driving conditions, traffic law enforcement

Stellenbosch University ethics approval number: ING-2017-1626

Uittreksel

Regoor die wêreld is nommerplaatherkennings-tegnologie (NPH) gebruik om voertuigverwante misdaad in stedelike gebiede te bekamp. Kommersiële beskikbare NPH-stelsels is egter duur en nie haalbaar vir grootskaalse aanneming in ontwikkelende lande nie. Die ontwikkeling van 'n laekostestelsel vereis 'n ingeligte benadering tot die keuse van 'n gepaste kamera, sowel as 'n realistiese begrip van die stelsel se vermoë onder verskillende omstandighede.

Hierdie werk het die effek van opto-elektroniese- en omgewingsfaktore op die vermoë van voertuig-gemonteerde NPH-stelsels om lisensieplate korrek te identifiseer geondersoek. 'n Teoretiese NPH-kamera model was ontwikkel om die effek van verskillende kamera tipes te bestudeer, terwyl die effekte van beweging, oriëntasie en beligting in 'n reeks eksperimentele toetse geëvalueer was.

Die mees invloedryke opto-elektroniese faktore was uitgeken as fokus, brandpuntafstand en beeldsensor resolusie. Nommerplate kon teoreties oor 'n groot gebied herken word deur die gebruik van 'n vaste-fokus primêre lens saam met 'n hoë-resolusie beeldsensor. Verder, was herkenning belemmer tydens hoë-spoed draaibewegings, sowel as in gevalle waar nommerplate teen 'n hoek, groter as 45°, weg van die kamera georiënteer was. In nagtoestande kon retroflekterende nommerplate op 'n afstand herken word vergelykbaar met dié van die dagtoestande, terwyl aankomende hoofligte akkurate herkenning belemmer het.

Die opto-elektroniese model was nuttig bewys vir die keuse van 'n koste-effektiewe kamera, vir gebruik in 'n oopbron NPH-stelsel. Daarbenewens het die studie van omgewingsfaktore waardevolle insig voorsien rakende die beperkings van NPH-stelsels in verskeie omgewings- en verkeerstoestande.

Acknowledgements

Firstly, I want to thank my Lord. He alone has sustained and transformed me along this journey. He is good and deserves all praise!

Sincerest thanks is also extended to Prof Thinus and Mr Barnard, whose patience, insight and kindness not only made this work possible, but also facilitated much learning.

Also, thank you to Prof Herman Steyn for offering the use of a rate table for my experiments.

I am also very grateful towards the Southern African Transport Conference for kindly funding this research and providing an opportunity to publish part of it.

Lastly, I would like to thank my family and friends for encouraging me and helping me grow. I especially want to thank my mother for providing much-needed support and wisdom in difficult circumstances.

Publications

Part of this work has been published as follows:

M.C. Rademeyer, M.J. Booysen, A. Barnard, "Factors that influence the geometric detection pattern of vehicle-based licence plate recognition camera systems", *37th Southern African Transport Conference*, July 2018, Pretoria, South Africa

Contents

List of Figures

List of Tables

Nomenclature

Abbreviations

A/D	Analogue to Digital Converter
AoV	Angle of View (Horizontal component)
CAA	Critical Apparent Angle
CCD	Charge-Coupled Device
CDS	Correlated Double Sampling
CMOS	Complementary Metal-Oxide-Semiconductor
DoF	Depth of Field
DoFF	Depth of Field Far Boundary
DoFN	Depth of Field Near Boundary
EU	European Union
GRE	Geometric Recognition Envelope
IR	Infrared
ISO	International Organization for Standardization
JPEG	Joint Photographic Experts Group
LPR	Licence Plate Recognition
MP	Megapixel
OF	Optical Format
ROI	Region of Interest
SA	South Africa
USB	Universal Serial Bus

Optoelectronic Parameters

α_d	Diagonal angle of view
α_h	Horizontal angle of view
β	Licence plate horizontal apparent angle
C	Maximum allowable circle of confusion diameter
C_{factor}	Circle of confusion factor
d	Image sensor diagonal length
D_F	Depth of field far boundary
D_N	Depth of field near boundary
f	Lens focal length
H	Hyperfocal distance

N	Aperture f-number
R_{plate}	Horizontal licence plate resolution
$R_{plateMin}$	Minimum allowable horizontal licence plate resolution
R_{sensor}	Horizontal image sensor resolution
S_{ext}	Lens extension
S_{focus}	In-focus distance
S_{sensor}	Lens to sensor distance
w	Image sensor width

Environmental Parameters

$\dot{\theta}$	Camera angular velocity in degrees
ϕ	Degrees of slant distortion
r	Camera turn radius
v	Camera velocity

Glossary

These terms appear frequently throughout this document. A useful definition of each is provided.

Capture	Saving an image as a digital photograph.
Derived camera property	Parameter describing an aspect of the captured scene and derived from primary camera properties. Also referred to as a derived property.
Geometric recognition envelope	Metric used in the optoelectronic investigation to model the boundary of the recognition area. Abbreviated to GRE.
Incoming light	Light from the scene entering the camera.
Image	Portion of the scene projected onto the image sensor.
Primary camera property	Physical parameter of a camera responsible for how a scene is captured. Also referred to as a primary property.
Recognise	Correct identification of an entire licence plate number contained within a photograph. Also referred to as accurate or successful recognition.
Recognition accuracy	Overall ability of a vehicle-mounted LPR system to correctly identify licence plates.
Recognition area	Region in front of an LPR camera in which licence plates are correctly identify.
Scene	The environment in front of the camera viewed from the camera's perspective.

Chapter 1

Introduction

In 2018, an average of 139 vehicles were stolen in South Africa every day [1]. A further 44 vehicles were hijacked every day, mostly near urban centers. These statistics provide a glimpse into the reality of vehicle-related crime rampant in today's cities.

Many law enforcement agencies across the world have successfully employed licence plate recognition (LPR) technology to crack down on vehicle-related crime. Approximately 71% of American law enforcement agencies use LPR technology [2] and Australian highway patrols daily catch multiple unregistered vehicles using LPR systems mounted on their patrol cars [3].

However, developing countries are prevented from harnessing the benefits of large scale LPR deployment due to commercially available systems generally being expensive, heavily reliant on proprietary technology and only offered as part of extensive solutions. In such countries, a scalable low-cost open source LPR system would enable the crowdsourcing of traffic monitoring to civilian vehicles. This would facilitate the use of civilian vehicles as 'eyes on the road' and greatly contribute towards community safety and effective law enforcement in developing countries.

Development of such a system would require an informed selection of an appropriate camera for use with readily available hardware and software. Additionally, the expected performance of such a system in various conditions should be established.

1.1 Research Question

This work will investigate how, and to what degree, (1) optoelectronic and (2) environmental factors affect the overall ability of vehicle-mounted LPR systems to correctly identify licence plates. This ability will be referred to as the system's recognition accuracy.

Optoelectronic factors were evaluated due to the vast range of compact cameras eligible for use in LPR systems. The investigation into environmental factors was motivated by the highly dynamic and unpredictable nature of urban traffic conditions. Such an study would provide insight into how environmental conditions and choice of camera affect recognition accuracy.

1.2 Objectives

Two primary objectives were identified. Each pertained to an investigation of multiple optoelectronic or environmental factors affecting recognition accuracy.

1. Identify and quantify the effect of **optoelectronic factors** on recognition accuracy
    a) Develop a theoretical model to estimate the effect of individual optoelectronic factors on recognition accuracy.
    b) Validate the accuracy of the model using empirical real-world results
2. Identify and quantify the effect of **environmental factors** on recognition accuracy
    a) Identify the type of motion predominantly responsible for affecting recognition accuracy. Determine the cause of limited recognition accuracy above certain velocities. Evaluate the effectiveness of correction techniques to enhance recognition accuracy in conditions involving such motion.
    b) Identify the most common orientation between vehicles in urban traffic. Determine at which point such orientation may limit recognition accuracy. Explore the use of correction techniques to enhance recognition accuracy in conditions involving such orientation.
    c) Determine how effects related to lighting conditions may influence recognition accuracy

1.3 Research Scope

This work did not consider the effect of different LPR algorithms. Such algorithms have been the focus of much research, with many reliable algorithms currently available. Likewise, various techniques exist to address or mitigate common recognition challenges [4, 5, 6]. Instead, this work focussed on understanding the origin of common limitations and how optoelectronic and environmental factors fundamentally affect the system's recognition accuracy.

A limited number of factors were investigated. This specifically included optoelectronic factors affecting the region in which licence plates are accurately recognised, as well as environmental factors, including motion, orientation and lighting.

The analysis specifically considered the application of a dashboard-mounted system operating in an urban traffic environment. Such an environment exhibits significant variation in vehicle movement and provided a comprehensive platform for the evaluation of environmental factors affecting recognition accuracy.

1.4 Document Structure

Chapter 2 provides an overview of existing LPR technology along with a detailed discussion of optoelectronic fundamentals and environmental factors prevalent in urban

traffic. Chapter 3 furthers the investigation into optoelectronic factors by presenting the development and validation of a theoretical model. A comprehensive mathematical framework provides an estimation of how different optoelectronic factors affect recognition accuracy. Chapter 4 covers the investigation into environmental factors by detailing the configuration of experimental tests and providing a discussion of the phenomena observed. Where possible, trends are applied to real-world traffic scenarios and correction techniques are demonstrated. Chapter 5 concludes this work by revisiting the initial research objectives. This is followed by a summary, as well as a discussion of possible future work and closing remarks.

Chapter 2

Literature Review

This chapter contains a summary of existing LPR technology, a discussion of optoelectronic fundamentals and an overview of common environmental factors affecting LPR systems.

2.1 Licence Plate Recognition

Licence plate recognition technology is employed throughout the world to identity motor vehicles. An LPR system comprises a digital camera, which captures a scene containing the licence plate, and a processing unit with a recognition algorithm, which is used to extract the licence plate characters from the photograph [7]. These systems are used in automatic speed enforcement, neighbourhood security, vehicle theft management and many other related scenarios that require vehicle identification.

2.1.1 Existing Systems

An LPR system can be mounted in a static position to monitor vehicles driving past a specific location, such as a free-flow highway toll plaza or an access gate [8]. Such systems are generally permanent installations, having a dedicated lane or area to monitor and making use of sensors to detect the presence of vehicles. LPR systems are also commonly mounted on board vehicles, typically on the dashboard, windshield or roof, as shown in Figure 2.1. This configuration allows licence plates to be recognised while the vehicle drives through traffic and facilitates the monitoring of an extensive road network [9].

Figure 2.1: Example of a roof-mounted LPR camera [10]

Commercial LPR systems can offer accurate recognition up to a range of 30 m, although this varies greatly depending on the quality of the components [11]. Some systems are capable of recognising licence plates travelling at speeds up to 250 km/h [12]. These metrics help describe recognition accuracy, and as such are important considerations when selecting an appropriate LPR system.

Recognition Algorithm
There is a large range of LPR algorithms available for use. Some high-end packages are proprietary and require a once-off payment or subscription fee in exchange for a highly optimised recognition algorithm [13, 14], while others are open-source and free [15, 16]. The typical algorithm consists of four basic stages: image acquisition and processing, licence plate detection, character separation and character identification [17]. The correct identification of an entire licence plate number contained within a photograph will be referred to recognition.

Image Acquisition and Processing
The recognition process starts with the capture of the scene by the image sensor. The photograph is saved as an image file and possibly compressed. At this stage, some algorithms apply image processing techniques to optimise the image for recognition [5].

Detection
After acquiring the image, it is scrutinised to detect the presence of any licence plates it may contain. This is commonly done by means of edge detection using the Canny, Sobel or Hough transform algorithms [6, 17]. These techniques all rely on the sharp contrast between the licence plate's light background and dark border to identify potential licence plates. These areas are labelled as regions of interest (ROIs) and passed on to the next stage. It should be noted that due to other objects in the scene also resembling the appearance of licences plates, not all detected ROIs will be licence plates.

Character Separation
Once an ROI has been identified, each character within it is isolated in preparation for individual recognition. This is commonly achieved by the projection technique, in which the intensity of each pixel in the ROI is projected onto a horizontal axis [17, 18]. The light-coloured spaces between characters will produce peaks along this axis, indicating character boundaries. Alternatively, the connected domain approach may be used to separate characters based on their uninterrupted outline [19]. Both these techniques are dependent on adequate contrast between the licence plate background and characters.

2.1.1.1 Character Identification

Lastly, the individual character images are classified. The character image may first be normalised by cropping away any white edges surrounding the character and rescaling it to a certain size [17]. The resultant image then undergoes template matching, in which it is compared to a database of character images. Such a database contains images of licence plate characters taken in various conditions and from different perspectives, and will be specific to a regional licence plate style. This process is repeated for each character, resulting in the entire licence plate number being output as a single text string.

2.2 Optoelectronic Fundamentals

A digital camera is considered an optoelectronic system because it manipulates and electronically captures light. This section will discus the various physical components of a camera involved when taking a photograph. Such components will be referred to as primary camera properties and greatly affect the resultant photograph. Attributes of the resultant photograph are also explored and will be referred to as derived camera properties.

2.2.1 Primary Camera Properties

The primary camera properties largely determine how a photograph is taken. Figure 2.2 shows a simplified camera, and illustrates how an object is projected onto the camera image sensor.

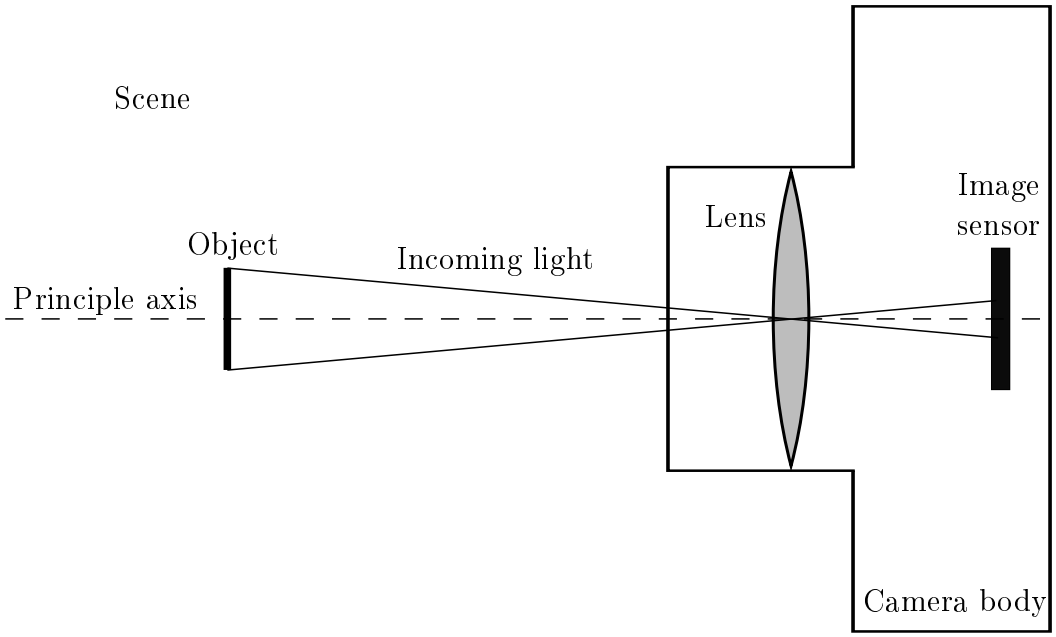

Figure 2.2: Diagram demonstrating the projection of an object onto the image sensor.

The direction in which a camera is aimed is referred to as its principle axis. The environment in front of the camera, viewed from the camera's perspective, is called the scene. Light from objects within the scene enter through the camera lens, and is projected onto the digital image sensor. This projected light is referred to as an image and is electronically captured to produce a digital photograph. Some of the more influential primary properties include focal length, distance between the lens and image sensor, the image sensor itself and exposure settings.

2.2.1.1 Focal Length

Focal length is an inherent property of each camera lens and describes to what degree the lens bends incoming light from objects within the scene. It is measured as the distance in millimetres (f) at which a lens concentrates light from an object infinity far away, as illustrated in Figure 2.3 [20]. Light from closer objects will concentrate further away from the lens.

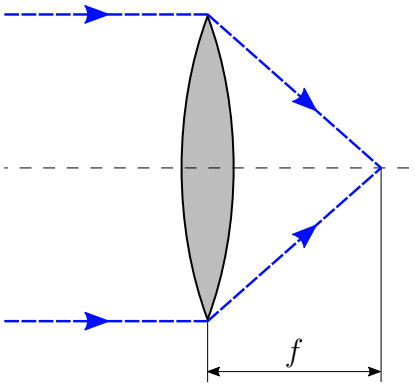

Figure 2.3: Light from an object infinitely far away converging at a distance equal to the lens focal length

A lens with fixed focal length is referred to as a prime lens. However, zoom lenses employ a combination of individual movable lenses to manipulate the overall effective focal length [20]. The zoom factor is equal to the maximum effective focal length divided by the minimum effective focal length. Commercial LPR cameras commonly employ zoom lenses with a focal length range suited to a specific application [11, 12, 21]. Some of these zoom lenses are motorised, while others have to be configured manually.

2.2.1.2 Lens to Sensor Distance

Objects are captured in sharp focus when their incoming light is concentrated precisely on the image sensor [22]. This is the case for objects at a specific distance, defined as the in-focus distance (S_{focus}). A desired in-focus distance is achieved by appropriately adjusting the distance between the lens and image sensor (S_{sensor}), as illustrated in Figure 2.4.

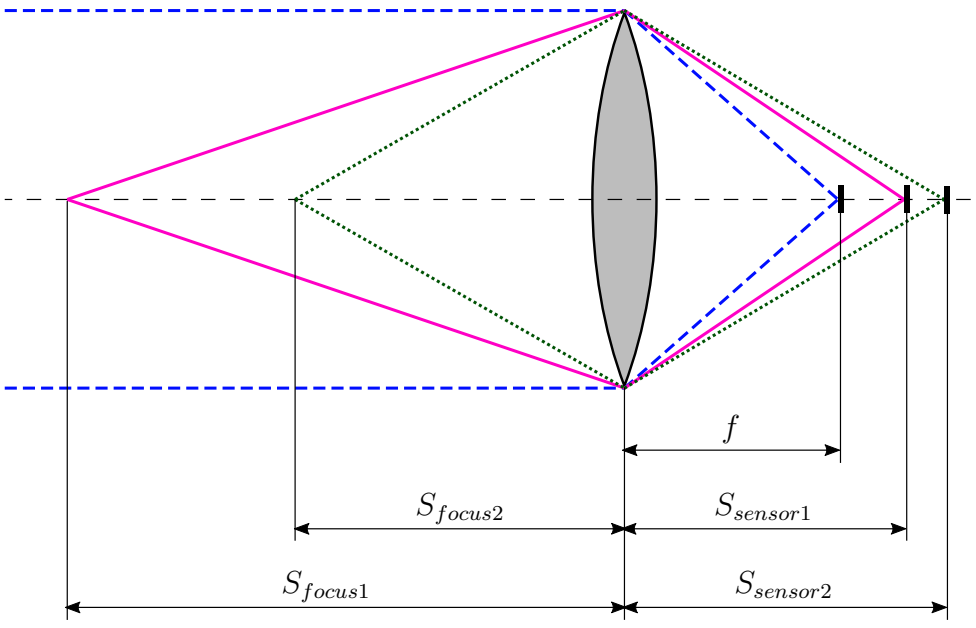

Figure 2.4: Illustration of a lens bending incoming light from objects at various distances. By adjusting S_{sensor}, light from an objects at a specific distance (S_{focus}) will be concentrated on the image sensor, resulting in these objects being captured in-focus.

Extending the lens further away from the sensor will bring closer objects within focus. The relationship between S_{sensor} and S_{focus} is defined by the thin lens equation as shown in Equation (2.1) [23].

$$\frac{1}{S_{focus}} + \frac{1}{S_{sensor}} = \frac{1}{f} \tag{2.1}$$

An adjustable focus lens allows the in-focus distance to be conveniently varied. Alternatively, fixed-focus lenses are static and posses a set in-focus distance, while auto-focus lenses automatically adjust the distance between the lens and sensor to keep objects within focus.

Zooming with a varifocal lens will result in a shifted in-focus distance and require that the camera be refocused after zooming. Parfocal zoom lenses do not present this issue.

2.2.1.3 Image Sensor

Light projected onto the image sensor is subsequently electronically captured by the image sensor. The image sensor is covered by an array of photosensors, each producing an electronic charge proportional to the intensity of light falling on it. This charge is sampled and converted into a digital image using either complementary metal-oxide-semiconductor (CMOS) or charge-coupled device (CCDs) technology.

CMOS sensors rely on photodiodes to convert incoming light into voltage [24]. The voltage over each photodiode is amplified by a connected CMOS transistor circuit, as shown in Figure 2.5a. The amplified voltage is sampled row-by-row by analogue to digital converters (A/Ds) situated at the end of each column [25]. A correlated double sampling (CDS) device removes any undesired voltage offset. CMOS sensors are commonly used for LPR due to their compact design and relative low cost and power consumption.

As an alternative, CCD sensors employ photosensitive capacitors which produce an electrical charge based on the amount of incoming light [24]. Image capture is achieved by each capacitor transferring its charge to the neighbouring capacitor, operating as a column shift register. This results in a single row of charges being ejected into a readout register at either the top or bottom of the sensor, as shown in Figure 2.5b. Charges in this register are sequentially amplified and sampled [25]. This entire process repeats until the full image has been captured. CCD sensors are commonly used in high-end video equipment due to their greater light sensitivity and lower noise levels [26].

The total number of photosensors on an image sensor is referred to as the resolution and is specified in megapixels (MP) or horizontal pixels by vertical pixels. A resolution of 1920x1080 is common in commercial LPR cameras [12, 21]. Large resolution generally corresponds to a large image sensor size. Sensor size is commonly classified as a type with unit of optical format inches (eg. a type 1/3.2" sensor). Use of this convention dates back to the use of vacuum tube imaging devices [27].

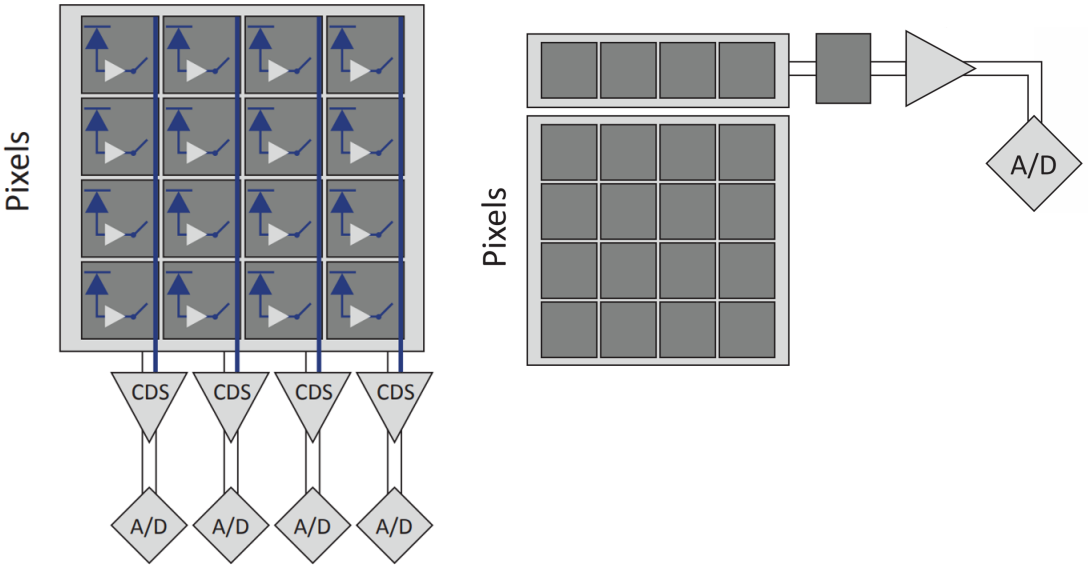

(a) CMOS sensor showing the individual amplifiers as well as the A/Ds situated at end of each column.

(b) CDD sensor showing the readout register and single amplifier and A/D.

Figure 2.5: Diagrams illustrating the basic components of a CMOS and CDD sensor sensor. (Simplified from [25])

To measure the colour of incoming light, the image sensor is covered by a colour filter array. A common example is the Bayer pattern, which consists of red, green and blue filters [26]. This has the effect of each pixel only absorbing one colour component. Based on the intensity and colour filter of each pixel, the full-colour image is interpolated by combining the different colour components.

2.2.1.4 Shutters and Effective Exposure

An image is captured by reading the amount of charge accumulated by photosensors within a specific period. Exposure time, also commonly referred to as shutter speed, is the duration for which each photosensor is exposed to incoming light. On the other hand, integration time is the duration for which each photosensor is electronically set to accumulate charge. The period for which a photosensor is both exposed and integrating is referred to at the effective exposure time [28].

There are two primary methods to control how long photosensors are effectively exposed, namely, global and rolling shutter [25]. In the case of global shutters, photosensors are permanently exposed. The image is captured by integrating all photosensors simultaneously, after which the image is read out. This allows the entire image to be captured as it appeared for a single moment in time. This method is used in frame-transfer and interline CCD sensors, as well as in some CMOS sensors.

Alternatively, rolling shutters stagger the starting time of effective exposure for each row of photosensors. This method is used in full-frame[1] CCD sensors, common in dig-

[1]Not to be confused with the 35 mm format sensor size also referred to as full-frame

ital single-lens reflex cameras, and is a inherent feature of the CMOS sensor readout method.

In a full-frame CCD sensor the effect of rolling shutter is commonly achieved by use of a focal plane shutter. This is a mechanical device that moves a pair of blinds down over the image sensor, one following the other. The horizontal gap between the blinds allow a slit of incoming light to move across the sensor, exposing photosensors. This action occurs while the entire sensor is integrating. The effective exposure time can be adjusted by changing the width of the gap and speed at which it moves.

The use of rolling shutter in CMOS sensors is referred to as progressive scan and is demonstrated in Figure 2.6. In this method, photosensors are permanently exposed and the intergeneration of each row starts as soon as the previous row has been read out. This allows image frames to be captured in rapid succession. The delay between the start of each row's effective exposure is equal to the row readout delay and is determined by the A/D speed.

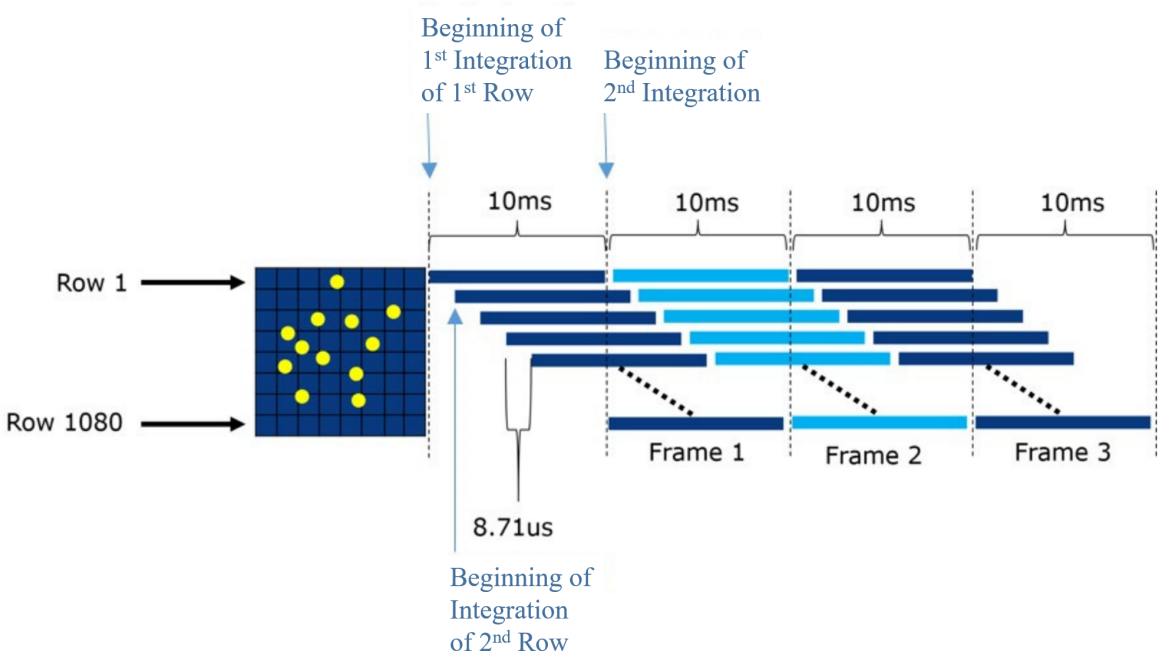

Figure 2.6: Timing diagram of a progressive scan shutter capturing three images sequentially. In this example, the integration time is 10 ms and the readout delay is 8.71 µs per row. (Adapted from [25])

Rolling shutters are renowned for causing slant distortion when used for the capture of fast moving objects. This is due to the delay between effective exposure of sequential rows. Slant distortion is further discussed in Section 2.3.1.2 on page 14 as part of the effect of relative motion within the scene.

2.2.1.5 Exposure Settings

In a broader sense, exposure refers to the amount of light captured when taking a photograph [29]. Using the correct exposure setting will ensure that the image is suf-

ficiently bright and that detail from the scene is captured. A camera's exposure is governed by the so-called exposure triangle of aperture size, shutter speed and ISO speed. All three these settings are adjustable and, in some cameras, are automatically set to ensure optimal exposure.

Aperture size
The camera aperture physically restricts the amount of light entering the camera [29]. The aperture size can be adjusted by varying the f-number setting. The diameter of the aperture opening will be equal to the focal length divided by the selected f-number. A large f-number will therefore imply a small aperture opening for a given focal length, allowing less light onto the image sensor. The range of available F-numbers are standardised so that each interval, referred to as an f-stop, will either double or halve the amount of incoming light.

Shutter speed
As discussed in a previous section, shutter speed determines the duration for which light is projected onto each photosensor before the image is captured [30]. As with aperture, shutter speed values are standardised such that each interval will either double or halve the exposure time, and effectively the amount of charge accumulated. The same effect is achieved by adjusting the integration time of a permanently exposed sensor, such as one using progressive scan.

Longer effective exposure is used in low-light conditions to allow a sufficient amount of charge to be accumulated. However, any movement of incoming light will result in light spreading over additional photosensors. Motion blur is produced when such movement occurs during effective exposure. A slower shutter speed, or longer integration time, will result in a greater amount of light movement being captured, thereby producing a greater effect of motion blur. Motion blur will be discussed in greater detail in Section 2.3.1.1 on page 13 as an effect of relative motion.

ISO speed
Lastly, ISO speed is the image sensor's sensitivity to light and is termed after the International Organization for Standardization, which defined it [31]. It effects the degree to which the camera electronically amplifies the charge generated by incoming light. High ISO speeds provide greater amplification, but also introduce additional noise in the captured image.

2.2.2 Derived Camera Properties

The captured image will exhibit certain characteristics based on the primary camera properties used to produce it. Such characteristics, or derived camera properties, included angle of view, depth of field and object resolution.

2.2.2.1 Angle of View

The angle of view (AoV) is the solid angle describing the portion of the scene captured by the camera. A wide AoV captures a greater area of the scene, while a narrow angle of view produces a zoomed-in image of a small area within the scene. A large AoV, such as produced by a fisheye lens, gives rise to the phenomenon of barrel distortion. This

poses a problem for LPR due to the rectangular frame of the licence plate becoming distorted in the captured image.

The AoV measured diagonally across the scene (α_d) is dependent on the image sensor diagonal (d) and focal length (f), as shown in Equation (2.2) [23].

$$\alpha_d = 2 \arctan\left(\frac{d}{2f}\right) \tag{2.2}$$

2.2.2.2 Depth of Field

Only objects located at the in-focus distance will be captured in sharp focus. However, objects can still be captured in sufficient focus in the region surrounding the in-focus distance. This is referred to as the depth of field (DoF) [22]. When positioned within the DoF, light from the object no longer concentrates perfectly on the image sensor, but slightly in front or behind it, as illustrated in Figure 2.7. This results in points of light from the scene being projected as large circles, referred to as circles of confusion.

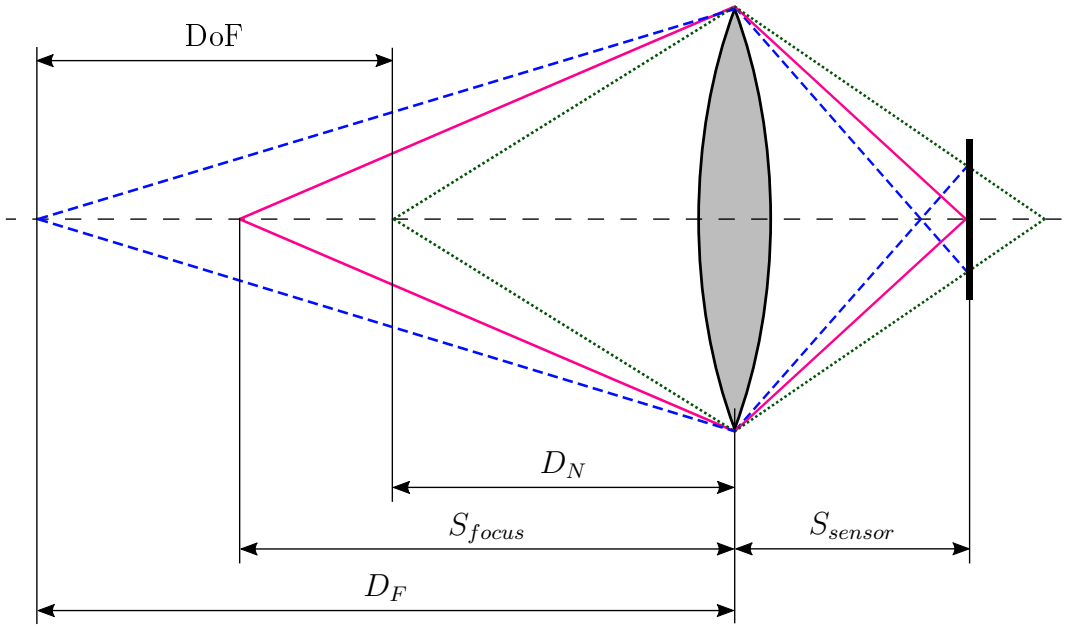

Figure 2.7: Illustration of the DoF. It is noteworthy that only light from objects positioned at S_{focus} (solid line) will be concentrated precisely on the image sensor.

The size of the depth of field is determined by a near (DoFN, D_N) and far (DoFF, D_F) boundary. The distance to each boundary can be calculated based on the in-focus (S_{focus}) and hyperfocal (H) distances, as shown in Equations (2.3) and (2.4) [32].

$$D_N = \frac{HS_{focus}}{H + S_{focus}} \tag{2.3}$$

$$D_F = \frac{HS_{focus}}{H - S_{focus}} \tag{2.4}$$

The hyperfocal distance is equal to the in-focus distance producing the largest DoF. The DoFF will approach infinity for any in-focus distance greater than or equal to

the hyperfocal distance. The hyperfocal distance can be calculated based on the focal length (f), aperture size in f-number (N) and maximum allowable circle of confusion diameter (C), as shown in Equation (2.5) [32].

$$H = f + \frac{f^2}{NC} \tag{2.5}$$

2.2.2.3 Object Resolution

Object resolution describes the number of pixels representing individual objects within the scene. Incoming light from the scene will cover an area of the image sensor proportional to the apparent size of each object within image. Depending on the sensor resolution, this area will cover a certain number of photosensors, each producing a pixel in the captured image. In the context of LPR, licence plates consisting of minimum 30 pixels in height can be accurately recognised, depending on the algorithm used [33].

2.3 Environmental Factors

Recognition accuracy is also influenced by the environment in which LPR systems operate [34]. Vehicle-mounted systems are subject to additional factors, which can generally be controlled in static applications. Three of the factors, namely relative motion, relative orientation and lighting, constantly change throughout the operation of a vehicle-mounted system, and are known to impact recognition accuracy [33]. In contrast, the influence of environmental factors are controlled or at least relatively constant in a static application, as in the case of a boom gate with mounted spotlight.

Environmental factors are present within the scene and not under the direct control of the camera system. Their effect is therefore preserved in the captured image and can generally be characterised by the resultant distortion. Each type of distortion poses a unique challenge to the recognition algorithm.

2.3.1 Relative Motion

In the dynamic environment of vehicle-mounted LPR, both camera and licence plates constantly change speed and move across on the road. When a camera and licence plate move at different velocities or trajectories the effect of relative motion is captured by the camera. Two common distortions resulting from relative motion are motion blur and slant.

2.3.1.1 Motion Blur

Motion blur typically occurs when moving objects are captured in low-light conditions, as shown in Figure 2.8. This is due to the longer effective exposure needed to capture a sufficient amount of incoming light. However, a object with relative motion will result in incoming light moving across the image sensor and spreading over additional photosensors. If this occurs during effective exposure, the moving object will appear as a streak in the captured image, a phenomenon referred to as motion blur.

Figure 2.8: Example of motion blur in low light conditions [35]

The amount of motion blur relates to the distance moved by incoming light during the effective exposure. As such, the amount of motion blur will be great when using a long effective exposure or capturing objects with high relative velocity. In CMOS sensors, this occurs when using a long integration time.

The motion blur is problematic for LPR due to the blur of licence plate and character edges. The lack of sharp, high-contrast edges severely limits the accuracy of the recognition algorithm. This effect is dependent on the amount of motion blur and can range from being negligible to rendering the captured licence plate completely unrecognisable. Various techniques have been developed to accurately recognise moderately blurred licence plates.

2.3.1.2 Slant Distortion

Another effect of relative motion, known as slant, occurs when a camera with a rolling shutter captures a licence plate moving horizontally across the scene. Due to the time difference between effective exposure of each sequential row of photosensors, each row will capture the licence plate an instant after the previous row. A rapidly moving licence plate will therefore appear to progressively shift in sequential rows. When stacked together in the final image, this shifting results in a slanted licence plate. If sensor readout starts with the top row, a licence plate moving to the right of the scene will exhibit slant to the left within the captured image.

The amount of slant will be great when a licence plate moves across the scene at high speed and a significant delay exists between the start of each row's effective exposure. In progressive scan CMOS sensors, this delay is coupled to the row readout speed and is determined by the A/D sampling frequency. A high-resolution sensor would further amplify the amount of slant due to the larger number of photosensor rows having to be read out during each image capture.

The slanting of licence plate characters pose a problem for character segmentation dependent on the projection technique. When projecting pixel intensity to the horizontal axis, the white spaces between characters on a slanted licence plate will produce narrower bands due to overlapping of characters and spaces. Furthermore, the char-

acter recognition stage will be unable to accurately match severely slanted characters. The issue of slant can be addressed with slant correction, which aligns the side edges of the licence plate with the vertical axis.

2.3.2 Relative Orientation

The relative orientation of the licence plate and camera also influences the recognition accuracy. A licence plate not precisely aligned towards the camera lens will result in a distorted licence plate shape being captured. This is referred to as perspective distortion. The type of perspective distortion is related to the axis on which the licence plate is rotated away from the camera. Figure 2.9 shows examples of licence plates rotated on the yaw, pitch and roll axes.

(a) Yaw distortion (b) Pitch distortion (c) Roll distortion

Figure 2.9: Common examples of perspective distortion (adapted from [33])

In all these distortions the licence plate is stretched, squashed or rotated in some way. When sufficiently distorted, the algorithm will be unable to accurately recognised the licence plate. Commercial LPR systems can tolerate some perspective distortion, such as a yaw angle of 15° and a pitch angle of 30° [33].

Various techniques exist to correct perspective distortion before passing the image on to the recognition process. An image with minimal distortion may be remedied by applying a simple stretch algorithm, effectively restoring the ratio of the capture licence plate to the its original value, albeit with lower resolution. Cases involving multiple types of perspective distortion can be addressed by applying planar homography to precisely invert the perspective distortion found within the captured image [6].

2.3.3 Lighting Conditions

Urban driving occurs in many different lighting conditions. Common examples include an overcast morning, a sunny afternoon or twilight. Light intensity in these conditions are primarily dependent on weather and time of day. Additionally, artificial light sources may be used to illuminate the scene, such as streetlamps or vehicle headlights. These sources may be directional and produce light of a specific wavelength. This section will discuss lighting phenomena related to LPR.

2.3.3.1 Retroflection

To aid in night-time visibility, most licence plates consist of stencilled black characters pasted on a retroflective background. The background reflects light directed at the licence plate back towards the source. This produces a high contrast between the background and characters, effectively aiding in recognition. A camera mounted on the dashboard of a vehicle is ideally located to capture light retroflected from the vehicle headlights.

2.3.3.2 Infrared Lighting

In addition to the visible light ordinarily within the scene, some commercial LPR systems effectively use infrared (IR) lighting to aid in recognition [12][21]. This typically involves mounting IR lamps next to the camera and using a camera sensitive to IR light (achieved by removing the IR-cut filter).

This technique also relies on the retroflective characteristic of licence plates, but instead of producing a steady source of light, the IR lamp strobes the licence plate. This high-intensity light for a short duration results in a negligible light trail being projected onto the image sensor and minimises the effect of motion blur. The IR spectrum is employed mainly due to it being invisible to humans, allowing the lamp to strobe without blinding or distracting road users.

2.3.3.3 Lens Effects

Another common phenomenon is that of lens effects produced by bright light sources shining directly into the camera lens. Typical effects, such as lens flare and glare, manifest as visible artefacts within the image. Lens flare occurs as a result of internal reflection within the camera. This is more common in zoom lenses, due to their multiple lens structure. Glare is displayed as a star-shaped haze surrounding the light source itself, generally exceeding it in size. These effects are often quite dramatic and can obscure detail within the scene.

Chapter 3

Optoelectronic Factors

This chapter details the investigation into the effects of optoelectronic factors on the recognition accuracy and specifically considers a forward-facing dashboard-mounted LPR camera. This analysis was conducted in a static and well-lit environment, allowing the impact of optoelectronic factors to come to the forefront. The region in front of the camera in which licence plates can be correctly identified was selected as a major aspect of recognition accuracy and defined as the recognition area. A theoretical model was developed to simulate the effect of primary camera properties on the recognition area, followed by an experiment to validate the simulated results.

3.1 Model

A mathematical model would afford the opportunity to evaluate many more camera properties than practically feasible. Creation of the model started by identifying the photographic conditions necessary for successful recognition. Each of these conditions were subsequently described in terms of a derived camera property and combined into a single metric. A theoretical framework was formulated to calculate the value of derived properties based on primary camera properties using fundamental optical formulas. Finally, the entire model was implemented as a software simulation.

3.1.1 Recognition Requirements

Certain photographic criteria have to be satisfied for a licence plate to be recognisable. Three of these were considered in the mathematical model, namely that the licence plate should be:

1. Wholly visible
2. Sufficiently focused
3. Captured in sufficient resolution

The first condition is self-explanatory, as a partially visible licence plate would result in only some characters being recognised. Secondly, high contrast was required along character edges for accurate recognition to be possible. This necessitated that licence plates be captured sufficiently in-focus. Lastly, licence plates had to be captured in sufficient resolution for accurate character identification to be possible.

Each of these conditions corresponded to a respective derived camera property, namely AoV, DoF and object resolution. This allowed the photographic criteria to be redefined in terms of these properties. A licence plate would be considered recognisable if it was:

1. Contained wholly within the AoV
2. Located within the DoF boundaries
3. Consisted of a minimum number of pixels

3.1.2 Geometric Recognition Envelope

The geometric recognition envelope (GRE) was defined as the boundary of the region in which licence plates satisfied all three recognition requirements, and was used as the primary metric for the effect of optoelectronic factors on recognition area. Licence plates located within the GRE were classified as recognisable, as illustrated by the green rectangles in Figure 3.1. Likewise, licence plates located outside of the GRE were classified as unrecognisable and displayed as grey rectangles.

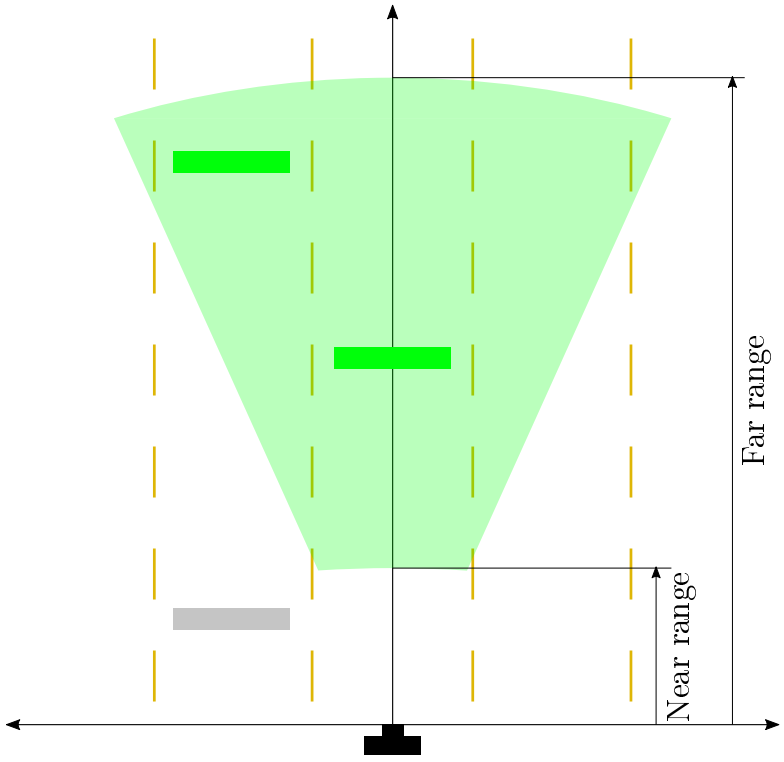

Figure 3.1: Example of a GRE being used to determine whether licence plates at different range and lane positions are classified as recognisable. The near and far recognition range is also indicated.

The shape of a GRE would be dependent on a camera's derived properties, and effectively described the estimated minimum and maximum recognition range, as well as the extent to which licence plates in adjacent lanes could be recognised. Use of the GRE metric would allow the model to be used as a tool for selecting an appropriate camera to achieve a desired recognition area. An LPR system with a large recognition area may lead to more licence plates being recognised while driving. However,

nearby vehicles may obstruct the camera's view and would thereby limit the effective far recognition range.

3.1.3 Theoretical Framework

A theoretical framework was formulated to calculate the derived camera properties based on primary properties describing the physical camera components. This would allow the GRE to be determined for any given camera.

3.1.3.1 Angle of View

The visibility requirement would be satisfied by licence plates located completely within the AoV. The horizontal component of AoV was used to determine whether all of a licence plate's characters were visible, as illustrated in Figure 3.2. The model used a typical licence plate width of 510 mm. The horizontal AoV also determined the extent to which licence plates in adjacent lanes were included within the GRE.

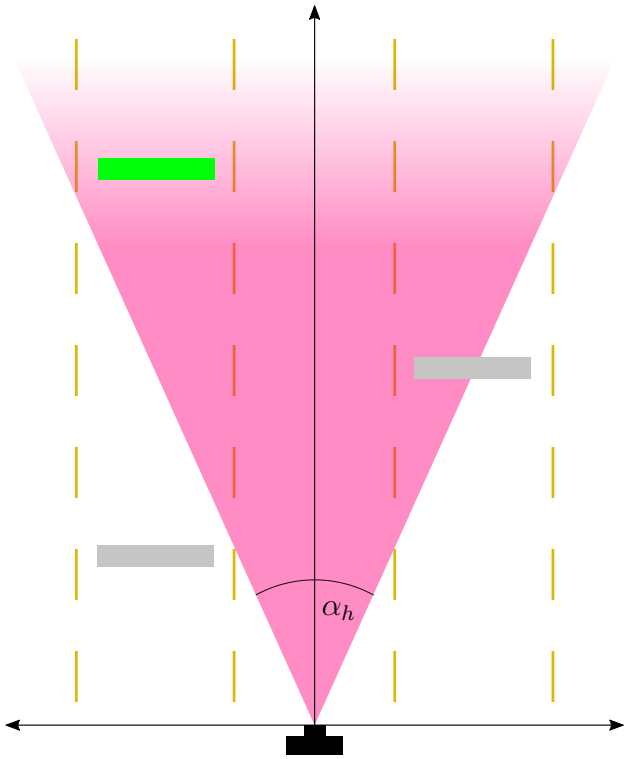

Figure 3.2: Illustration of how horizontal AoV determined whether all of a licence plate's characters were visible in the capture image.

The diagonal AoV equation (Equation (2.2)) was adjusted for horizontal AoV (α_h) by substitution image sensor width (w) for diagonal length, as shown in Equation (3.1). Hereafter, the term AoV will refer specifically to the horizontal AoV.

$$\alpha_h = 2 \arctan\left(\frac{w}{2f}\right) \tag{3.1}$$

The image sensor width was required in millimetres, to match the unit of focal length. However, sensor size is commonly classified as a specific type in optical format (OF)

inches. No exact standard exists for conversion of sensor type to a metric equivalent. As such, existing image sensors exhibit slight variation in size for a given type. This analysis used typical sensor dimensions, shown in Table 3.1. These sizes are specific to sensors with a 4:3 aspect ratio, which is common in compact image sensors.

OF (inches)	d (mm)	w (mm)
1/4	4.50	3.60
1/3.6	5.00	4.00
1/3.2	5.63	4.50
1/3	6.00	4.80
1/2.7	6.67	5.33
1/2.5	7.20	5.76

Table 3.1: Typical image sensor sizes in optical format inches, diagonal millimeters and width milimeters [27][36]

Using these values, the AoV could be calculated for any focal length and sensor type using Equation (3.1).

3.1.3.2 Depth of Field

Licence plates would be captured in sufficient focus for accurate recognition if located within the DoF boundaries, as illustrated in Figure 3.3.

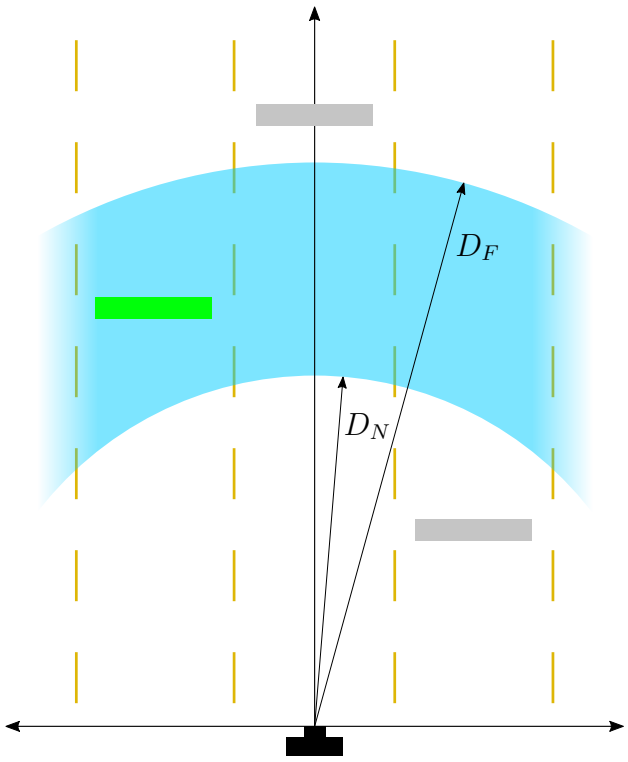

Figure 3.3: Illustration of how the near (D_N) and far (D_F) DoF boundaries determined whether licence plates were captured in sufficient focus for recognition.

As mentioned in Chapter 2, the near and far DoF boundaries are dependent on the in-focus (S_{focus}) and hyperfocal (H) distances as per Equations (3.2) and (3.3).

$$D_N = \frac{HS_{focus}}{H + S_{focus}} \tag{3.2}$$

$$D_F = \frac{HS_{focus}}{H - S_{focus}} \tag{3.3}$$

However, the in-focus and hyperfocal distances are not inherent camera properties, but rather are determined by the primary camera properties used to describe the physical components of a camera. As such, these two distances were referred to as intermediate properties and described them in terms of primary camera properties.

In-focus Distance

As discussed in Chapter 2, the in-focus distance is determined by the distance between the lens and image sensor (a primary camera property). As illustrated in Figure 3.4, an infinity far away focus is achieved when the image sensor is positioned at a distance to the lens equal to the focal length (solid line). Extending the distance between the lens and image sensor past the focal length would produce a nearer in-focus distance (dashed line).

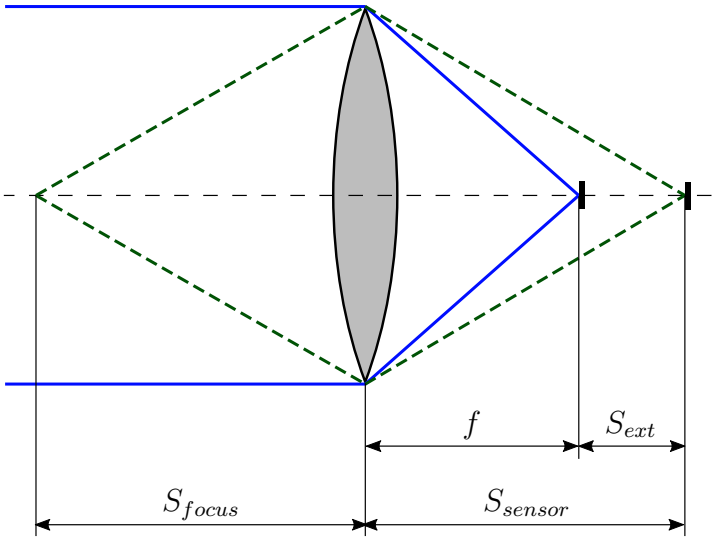

Figure 3.4: Illustration of S_{sensor} being extended past the focal length, resulting in a closer in-focus distance.

The difference between S_{sensor} and f was defined as the lens extension (S_{ext}). This provided a new definition for S_{sensor}, shown in Equation (3.4). Such a definition would allow lens extension to be analysed independently of focal length, affording greater insight into the effect of the two individual properties.

$$S_{sensor} = f + S_{ext} \tag{3.4}$$

Substituting this definition into the thin lens equation (Equation (2.1)) provided a solution for S_{focus} in terms of two primary camera properties, as shown in Equation (3.5).

$$S_{focus} = \frac{f^2}{S_{ext}} + f \tag{3.5}$$

Hyperfocal Distance

As discussed in Chapter 2, the hyperfocal distance is dependent on the focal length, f-number and maximum circle of confusion diameter, as shown in Equation (3.6).

$$H = f + \frac{f^2}{NC} \tag{3.6}$$

The maximum circle of confusion diameter is a chosen threshold and not an inherent camera property. It is commonly described as a fraction (C_{factor}) of the diagonal image sensor size, as shown in Equation (3.7). The GRE model used a C_{factor} of 1500, as is commonly used in the photographic industry [37].

$$C = \frac{d}{C_{factor}} \tag{3.7}$$

This equation was substituted into the hyperfocal equation to provide a solution for hyperfocal distance in terms of primary camera properties and the selected circle of confusion factor, shown in Equation (3.8).

$$H = f + \frac{f^2 C_{factor}}{Nd} \tag{3.8}$$

The redefined in-focus and hyperfocal distance equations would allow the DoF to be calculated based on primary camera properties.

3.1.3.3 Object Resolution

Licence plates were required to occupy a minimum number of pixels for accurate recognition to be considered possible. The licence plate resolution would depend on both the sensor resolution, as well as the portion of the sensor covered by light from the licence plate. Based on this relationship, a single new requirement was created to detemine whether licence plates would be captured in sufficient resolution for recognition.

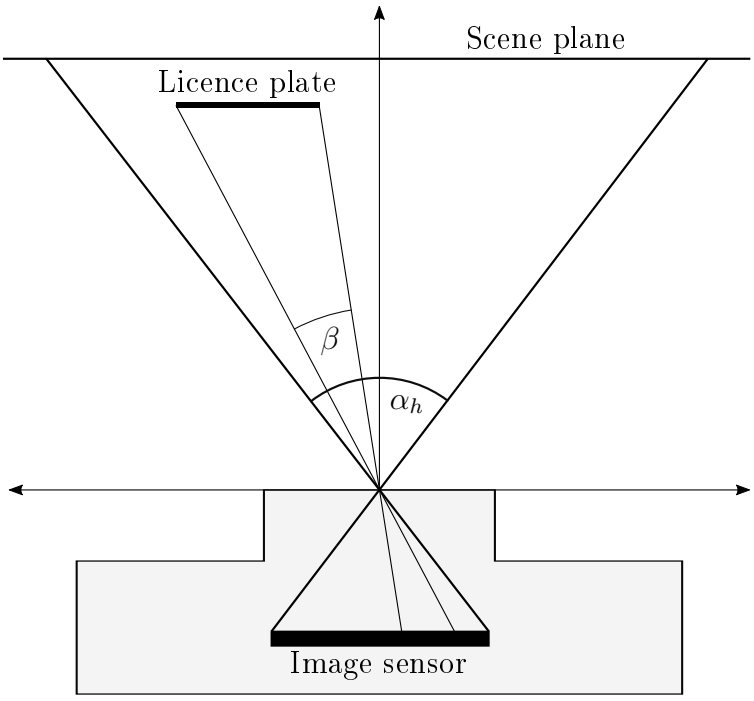

Figure 3.5: Illustration of perspective projection and licence plate apparent angle (β)

Figure 3.5 illustrates light from a licence plate within a scene being projected onto the image sensor based on the perspective projection model. This model describes the projection of light in a pin-hole camera, but may also be used for modelling conventional non-fish-eye lenses common in LPR cameras [38]. In this model, the scene may be approximated as a flat plane that is proportionally projected onto the image sensor. The angle formed between the side edges of a licence plate was defined as its apparent angle (β).

Due to the proportional projection of the scene, the licence plate's apparent angle divided by the AoV would be equal to the number of horizontal pixels it occupies (R_{plate}) divided by the total horizontal sensor resolution (R_{sensor}). This relationship is shown in Equation (3.9).

$$\frac{\beta}{\alpha_h} = \frac{R_{plate}}{R_{sensor}} \tag{3.9}$$

By setting R_{plate} equal to the minimum number of horizontal pixels required for recognition ($R_{plateMin}$), β would describe the critical apparent angle (CAA) which a licence plate should occupy for it to be captured in sufficient resolution.

$$\frac{CAA}{\alpha_h} = \frac{R_{plateMin}}{R_{sensor}} \tag{3.10}$$

The CAA could be applied to licence plates at any bearing from the camera and was used as the requirement for sufficient resolution, as illustrated Figure 3.6. Licence plate were considered to occupy sufficient resolution only if they exceeded the CAA, as shown by the two near licence plates.

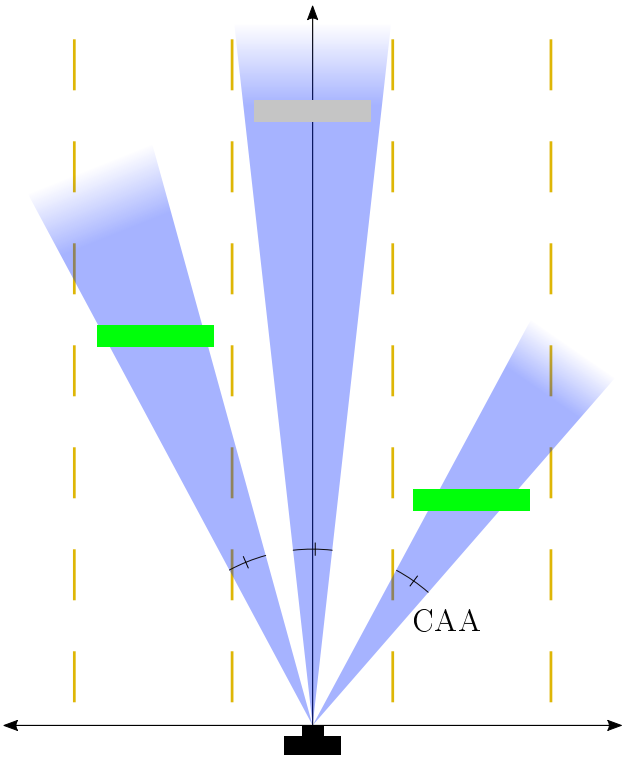

Figure 3.6: Illustration of how the capture of licence plates in sufficient resolution was determined based on whether licence plates exceeded the CAA.

The theoretical model used an $R_{plateMin}$ of 140 pixels, based on the common recognition requirement of 30 vertical pixels and the aspect ratio of European Union (EU) licence plates [33].

The CAA provided a single requirement for determining sufficient licence plate resolution, effectively incorporating sensor resolution, as well as the portion of the image occupied by the licence plate. A smaller sensor resolution or wider AoV would increase the CAA, effectively requiring licence plates to be nearer for accurate recognition.

3.1.3.4 Summary

The mathematical dependency of the derived properties on primary camera properties is summarised in Figure 3.7. The numbers in brackets indicate the equation by which each property could be calculated.

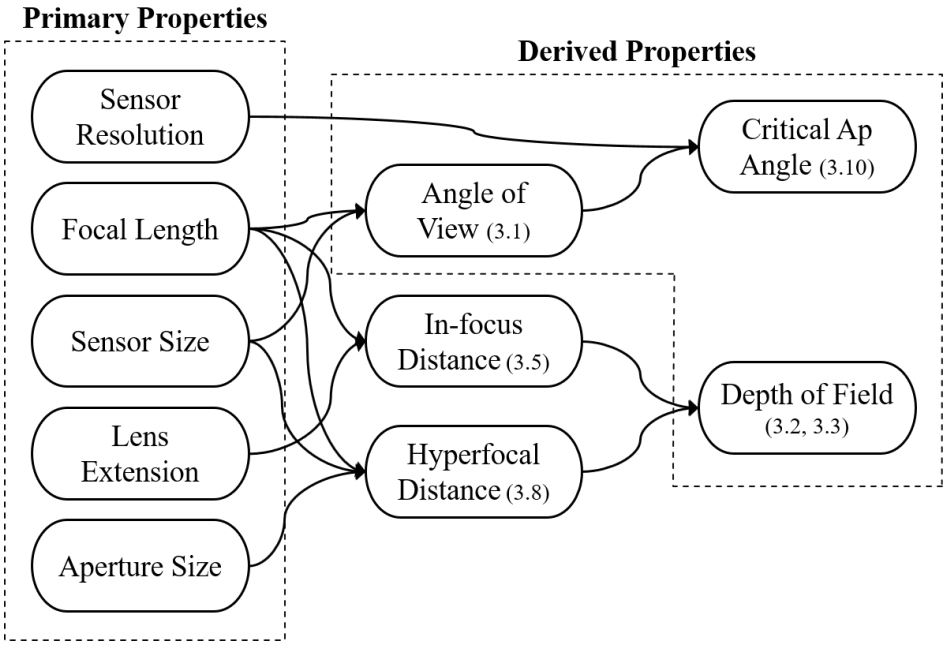

Figure 3.7: Mathematical dependency of derived camera properties on primary camera properties

The GRE would be the mutually inclusive region of the AoV, DoF and CAA, as illustrated in Figure 3.8 (the CAA is only shown for licence plates on a single bearing from the camera). The far range would be limited by either the CAA or the DoFF, while the DoFN would solely determine the near recognition range. Coverage of adjacent lanes would be governed by the AoV.

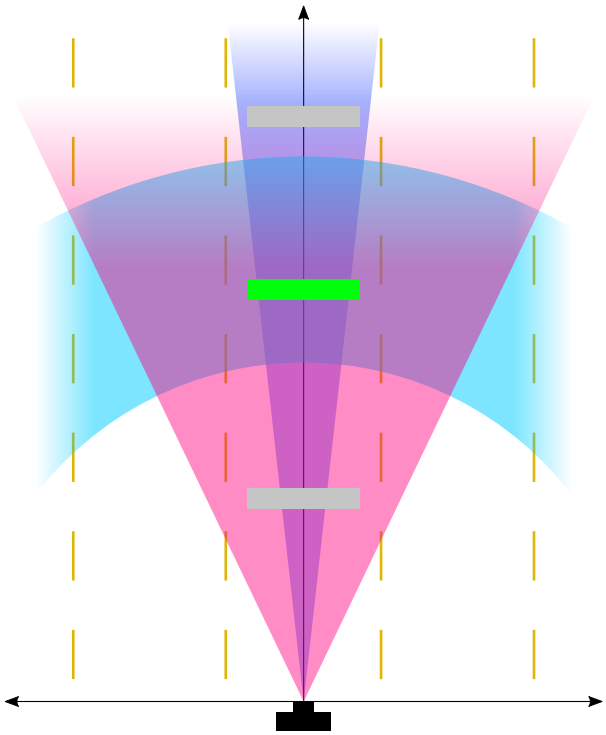

Figure 3.8: Illustration of how the AoV (red), DoF (cyan) and CAA (purple) determined the shape of the GRE and where licence plates were classified as recognisable.

3.1.4 Simulation

The theoretical model was implemented as a software simulation. Due to each derived property being dependent on multiple primary properties, it was necessary to consider the effect of all five primary properties in unison. For a given set of five primary property values, defined as a camera configuration, the corresponding derived properties were calculated and GRE determined. This was done for multiple camera configurations to provide insight into how each primary property affected the GRE.

3.1.4.1 Camera Configurations

In reality, the value of each primary camera property can be selected relatively independently of the others. There even exists some choice in image sensor size for a given resolution. In the simulation, this multidimensional problem was solved by identifying an appropriate range for each primary property and evaluating every possible camera configuration. Each range was based on values typically found in compact cameras and is shown in Table 3.2.

Camera property	Simulated range
Focal length	1 - 16 mm (0.5 mm increments)
Lens extension	0 - 22 µm (2 µm increments)
Aperture (F-num)	1.8, 2.0, 2.2, 2.4, 2.6, 2.8
Sensor resolution	0.5MP, 2MP, 5MP, 8MP
Sensor size	1/4", 1/3.6", 1/3.2", 1/3", 1/2.7", 1/2.5"

Table 3.2: Simulated primary camera property ranges

The aperture range was based on the one-quarter-stop f-number scale, in which each increment decreases the aperture size by approximately a quarter. The sensor resolution range represented resolutions of 800×600, 1600×1200, 2560×1920 and 3264×2448. The number of horizontal pixels in these resolutions approximated increasing multiples of 800, providing a linear scale for use in the simulation.

3.1.4.2 Plotting of the GRE

To appreciate the GRE of a vehicle-mounted camera, the GRE was plotted onto a virtual section of road, illustrated in Figure 3.9. This comprised three 3.5 m-wide lanes and a forward-facing camera in the middle lane.

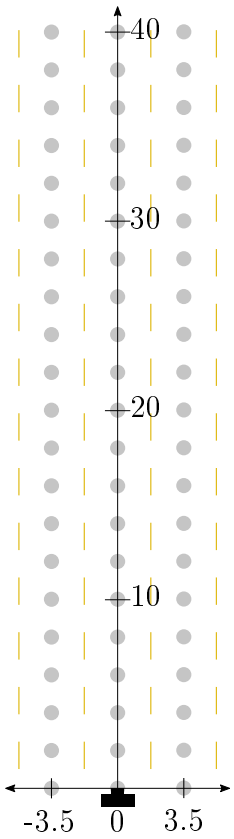

Figure 3.9: Illustration of the virtual road section used for plotting of the GRE

Such a configuration simulated a dashboard-mounted camera travelling in the middle lane of a three-lane single carriageway. The three lanes would incorporate same-direction, same-lane and oncoming traffic, although this analysis only considered static licence plate positions. The centre of each lane was finally discretised into positions spaced at 2 m intervals. This provided a useful comparative metric for the number of positions included in a given GRE.

The simulation produced a graphical representation of the GRE along with the derived properties which determined it. By varying a single primary camera property, its effect on the GRE and each derived property could be observed.

3.2 Experiment Setup

To validate the theoretical model, a real-world experiment was conducted to empirically determine the recognition area for different camera configurations. This was deemed necessary due to the complexity involved in accurately simulating the recognition area, as well as the limited usefulness of a purely theoretical model. Such an experiment would provide further insight into the effect of primary camera properties on recognition area, serve to validate the model, and reveal phenomena not included within the model.

The experiment entailed a licence plate being captured at multiple positions and the resultant photographs passed to a recognition algorithm. The recognition area was subsequently established based on the positions at which the algorithm correctly identified the licence plate. This involved an experimental camera, as well as computer hardware and software, and was conducted in a specific test environment.

3.2.1 Camera

The choice of experimental camera was guided by trends observed in the simulation. A camera with variable focal length and lens extension, as well as a high-resolution sensor, would be able to produce large variation in the GRE. Such variation would aid in identification and evaluation of the effects of individual primary camera properties. It also became clear that practical limitations existed in the choice of primary properties. Some property combinations are rare, such as a small image sensors with large resolution, while other properties, such as aperture, are only available in standardised sizes.

Incorporating the limitations of real world cameras, led to the selection of an experimental camera with properties shown in Table 3.3. The camera featured a CMOS sensor with a progressive scan shutter.

Property	Value
Focal length	2.6 - 9 mm varifocal
Lens extension	Manually adjustable
Aperture	f/1.8 max opening
Sensor resolution	3264×2448 (8MP)
Sensor size	1/3.2" (5.7mm diagonal)

Table 3.3: Primary properties of the experimental camera

The lens featured manual adjustment rings for variable focal length, aperture size and lens extension. This invaluable feature allowed the evaluation of different primary properties using a single camera, thereby maintaining a consistent test platform and minimising cost.

However, the manual adjustment rings were unmarked and thereby limited the accuracy to which properties could be set. Nevertheless, the limits of these variable properties were specified in the camera datasheet and the adjustment rings were turned to the extreme settings to produce these property values. This allowed two camera configurations to be evaluated, with the minimum and maximum focal lengths being used

together with the largest aperture size. Due to the use of a varifocal lens, the lens extension was readjusted for each configurations such that the majority of the test range would be in focus.

3.2.2 Computer Hardware

The experimental camera featured a universal serial bus (USB) interface for the transfer of captured images. This was connected to a Raspberry Pi 3 single-board computer, on which the experimental software ran. Raspberry Pi's are readily available in developing countries and offer sufficient processing power for the execution of a recognition algorithm. Furthermore, Raspberry Pi's are also suited for use in vehicle-mounted applications, due to their compact size and sufficiently low-power rating. The Raspberry Pi was remotely controlled from a laptop via an Ethernet connection. The photographs and recognition results were stored locally on a microSD card.

3.2.3 Software

The experimental software comprised three stages, namely image capture, recognition, and storage of the result, as shown in Figure 3.10.

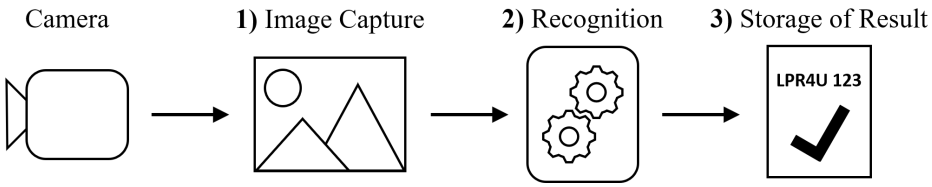

Figure 3.10: Process diagram describing the three stages of the experimental software

Image Capture
In the first stage, an image was captured by a webcam application interacting with the camera over the USB connection. The captured image was subsequently saved at full resolution and minimal compression, producing a very high quality image with a Joint Photographic Experts Group (JPEG) quality level greater than 95. This method was simple to implement and deemed sufficient for the preservation of image quality.

Recognition
The image file was subsequently passed to the recognition algorithm. The OpenALPR algorithm was used due to it being freely available[1], widely supported and reliable. On average, the algorithm took 3.6 seconds to recognise a licence plate in an 8MP image.

The algorithm was implemented as a plug-and-play module and not modified in any way. The use of a stock algorithm served as consistent recognition accuracy baseline for use in various testing conditions. This allowed for the analysis of factors independent of recognition algorithm employed. Additionally, both algorithm classifier and licence plate employed the EU format. This mitigated any recognition challenges related to a mismatch of licence plate format and facilitated an investigation independent of licence plate format.

[1]The OpenALPR source code can be download from `https://github.com/openalpr/openalpr`

Storage of Result
Lastly, the OpenALPR recognition result were annotated with the primary camera properties and licence plate position before being stored on the microSD card. The entire process was repeated multiple times for a given camera configuration, with the licence plate being captured at various positions. Finally, the recognition area of a specific camera configuration was established based on the positions at which the algorithm correctly identified the licence plate.

3.2.4 Test Environment

The experiment was conducted at night in a large indoor venue. This afforded complete control over lighting conditions by eliminating varying ambient light entering through windows and allowing the use of consistent artificial light. Furthermore, there was no movement within the venue. This provided a test environment in which the effect of optoelectronic factors could be repeatedly evaluated.

A test range, identical to that used in the simulation, was plotted within the venue. The experimental camera was securely mounted on a tripod and kept stationary throughout the experiment. The licence plate was mounted on a movable tripod and placed at various positions along the centre of each lane, orientated perpendicular to the direction of travel. The tripods were of equal height to negate unwanted perspective distortion caused by capture of the licence plate from an elevated angle (the effect of perspective distortion is investigated in Chapter 4).

3.2.5 Limitations

The experimental camera's adjustment rings were expected to be inaccurate, even at the extreme settings. The focal lengths and aperture size considered were solely based on values claimed in the camera datasheet. Furthermore, the unmarked rings obscured the exact lens extension used in either camera configuration, while the use of a single image sensor offered only a fixed resolution and sensor size.

The lack of accurately adjustable primary camera properties limited the experiment to only two camera configurations, each with a different focal length. However, the use of a single camera did provide consistent properties across the two configurations, allowing the effect of focal length to be accurately identified.

Furthermore, the experiment employed a single recognition algorithm, thereby producing a recognition area dependent on the inherent strengths and weaknesses of the OpenALPR algorithm. The use of multiple algorithms may have cancelled out unique performance differences and produced a more generic recognition area.

3.3 Model Results and Discussion

The results were organised to illustrate the effect individual primary camera properties on the GRE. This entailed varying a single primary property while keeping the others constant. The constant properties were chosen to produce a set of GREs that fitted

within the test range and effectively demonstrated the effect of the property being analysed. The constant properties used for each analysis is contained in Appendix A.

3.3.1 Focal Length

A change in focal length affected all three derived properties and thereby the overall shape of the GRE. Figure 3.12 shows the simulated GREs, along with derived properties, for a range of focal lengths.

It is evident that an increased focal length produced a narrower AoV and enabled the recognition of licence plates at greater range. This corresponded to the inversely tangential decrease of AoV for an increasing focal length. It was further apparent that an increasing focal length caused the DoF to progress away from the camera, due to the in-focus and hyperfocal distances increasing. The CAA decreased proportionally to the shrinking AoV.

The DoFF was identified as the far range limiting factor for a focal length of 5 and 7 mm, as evident from the maximum GRE range matching the DoFF. However, for greater focal lengths, the maximum range of the GRE was closer than the DoFF, implying that far range was instead determined by the CAA.

This change was due to an increasing DoFF alongside a decreasing CAA. Both these trends allowed for greater far recognition range, due to further focus and a narrower allowable apparent angle, as illustrated in Figure 3.11. However, the DoFF changed at a greater rate than CAA, resulting in CAA becoming the far range limiting factor for focal lengths of 9 mm and up. At this point, the reason for limited far recognition changed from insufficient focus to insufficient licence plate resolution.

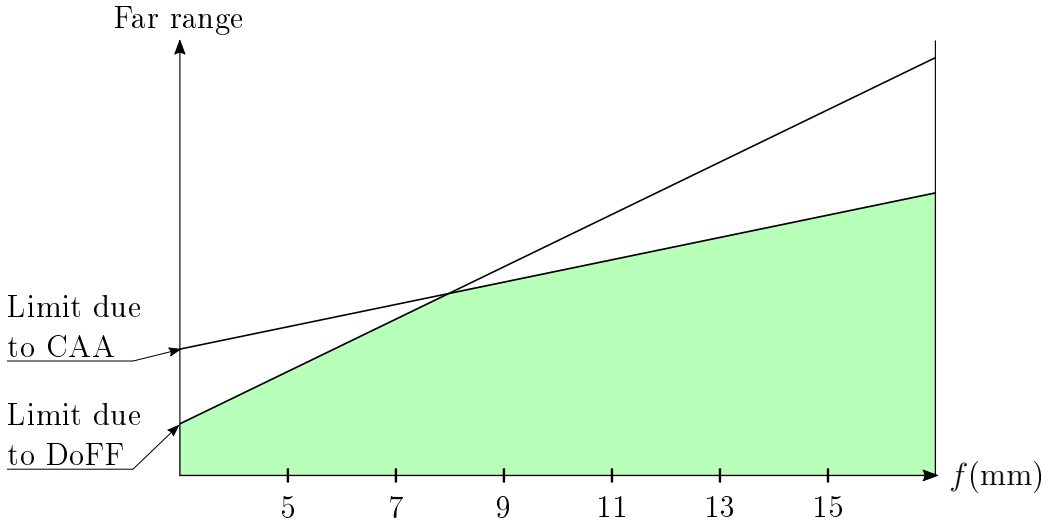

Figure 3.11: The relationship between CAA and DoFF as far range limiting factors for various focal lengths. The shaded region represents the GRE and is determined by the nearest limiting factor.

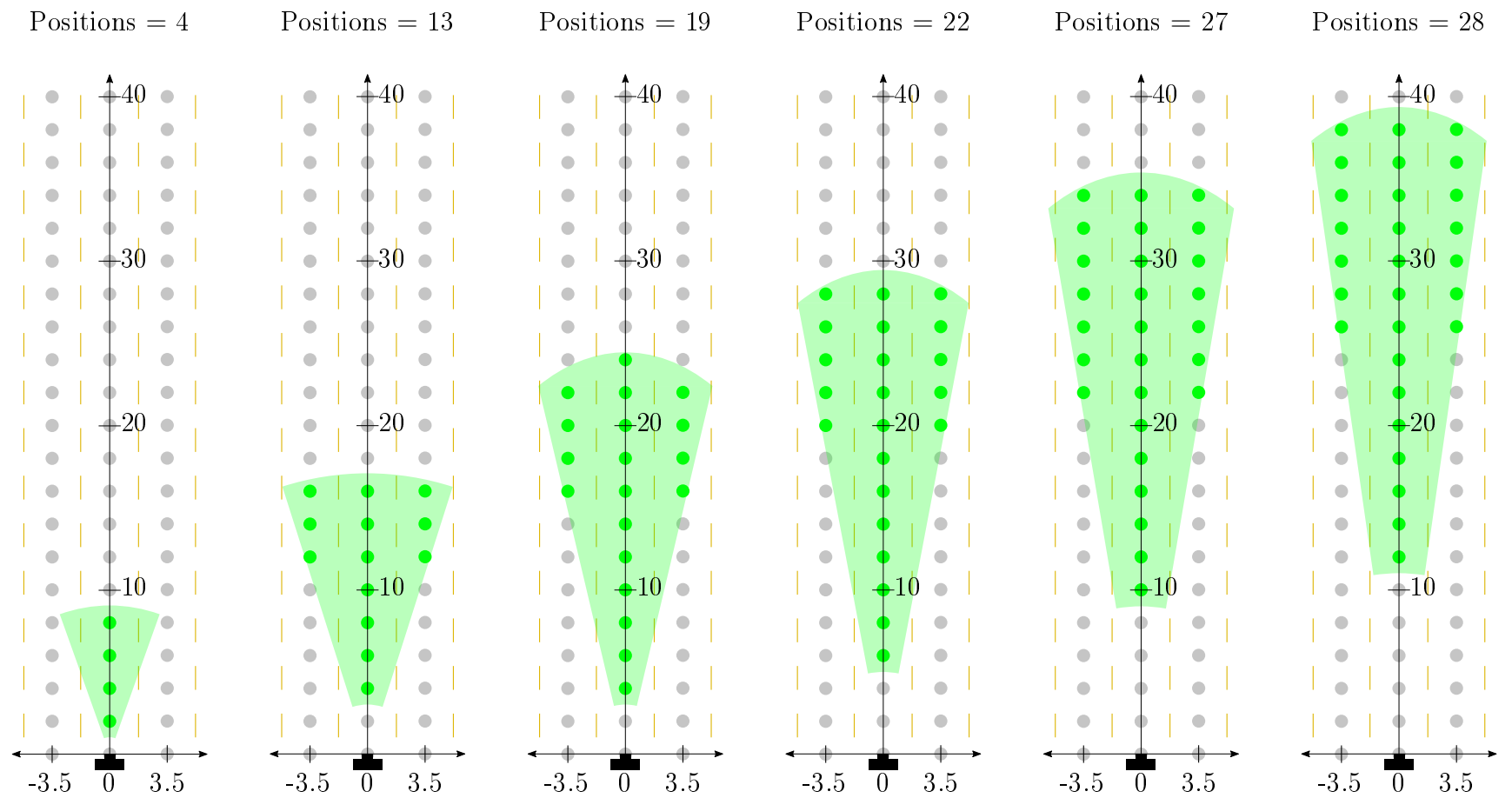

AoV	48.49°	AoV	35.67°	AoV	28.10°
DoFN	1.19 m	DoFN	2.33 m	DoFN	3.86 m
DoFF	8.39 m	DoFF	16.43 m	DoFF	27.14 m
CAA	2.080°	CAA	1.530°	CAA	1.205°
$f = 5\,\text{mm}$		$f = 7\,\text{mm}$		$f = 9\,\text{mm}$	

AoV	23.14°	AoV	19.66°	AoV	17.08°
DoFN	5.77 m	DoFN	8.05 m	DoFN	10.72 m
DoFF	40.52 m	DoFF	56.58 m	DoFF	75.31 m
CAA	0.993°	CAA	0.843°	CAA	0.732°
$f = 11\,\text{mm}$		$f = 13\,\text{mm}$		$f = 15\,\text{mm}$	

Figure 3.12: Simulated GREs and derived properties for various focal lengths (axis in meters)

3.3.2 Lens extension

Extending the lens further away from the image sensor brought the in-focus distance closer and thereby affected both DoF boundaries, as is evident in Figure 3.13. A lens extended 6 µm past the focal length produced a DoFF approaching infinity. A greater lens extension shortened both the DoFN and DoFF, and shrunk the overall GRE area.

It is noteworthy that a large GRE can be achieved for a single lens extension, as in the case of $S_{ext} = 14\,\mu m$. This indicates that the use of a fixed-focus lens may be sufficient for achieving a large recognition area. Such a lens will be a reliable and inexpensive alternative to an auto-focus lens.

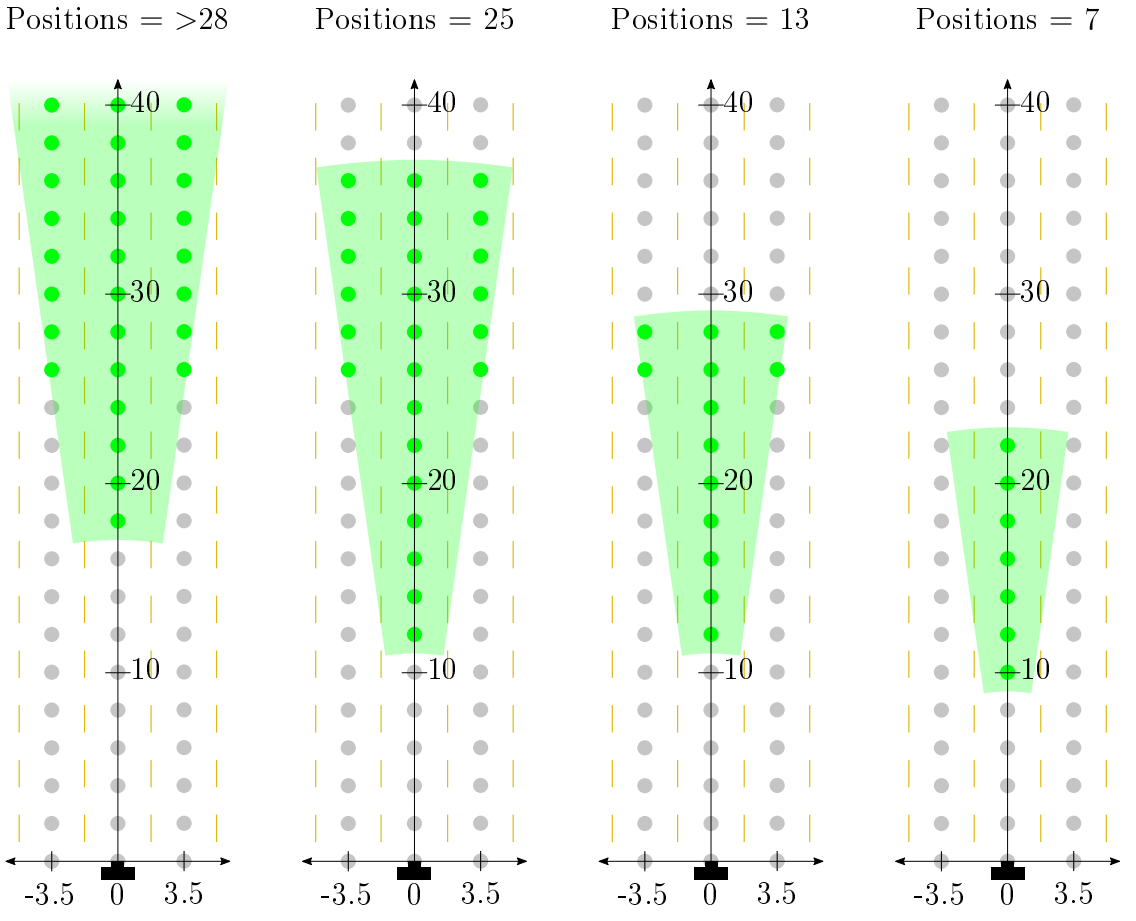

Figure 3.13: Simulated GREs and derived properties for various lens extensions (axis in meters)

3.3.3 Aperture Size

The aperture size affected the hyperfocal distance and thereby the DoF, as shown in Figure 3.14. An increasing f-number, corresponding to a smaller aperture opening, extended the DoFF and shortened the DoFN, producing a larger GRE.

It should be noted that a small aperture size would also decrease the overall exposure, a factor excluded from the GRE analysis. This could potentially impair recognition accuracy in low light conditions.

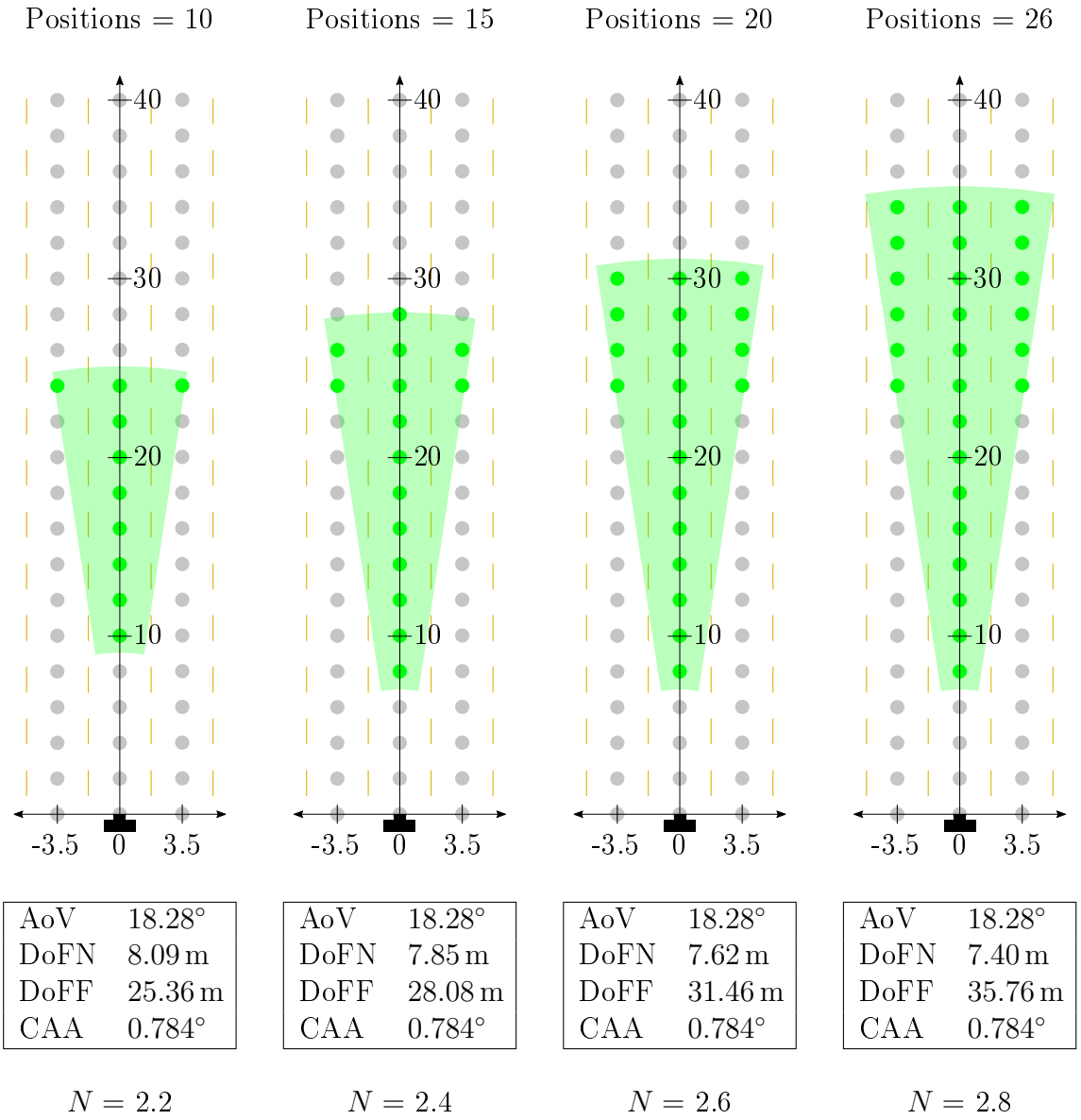

AoV	18.28°	AoV	18.28°	AoV	18.28°	AoV	18.28°
DoFN	8.09 m	DoFN	7.85 m	DoFN	7.62 m	DoFN	7.40 m
DoFF	25.36 m	DoFF	28.08 m	DoFF	31.46 m	DoFF	35.76 m
CAA	0.784°	CAA	0.784°	CAA	0.784°	CAA	0.784°
$N = 2.2$		$N = 2.4$		$N = 2.6$		$N = 2.8$	

Figure 3.14: Simulated GREs and derived properties for various aperture sizes in f-number (axis in meters)

3.3.4 Image Sensor Resolution

A increased sensor resolution inversely proportionally affected the CAA. The resulted in a dramatic extension of recognition range, as shown in Figure 3.15.

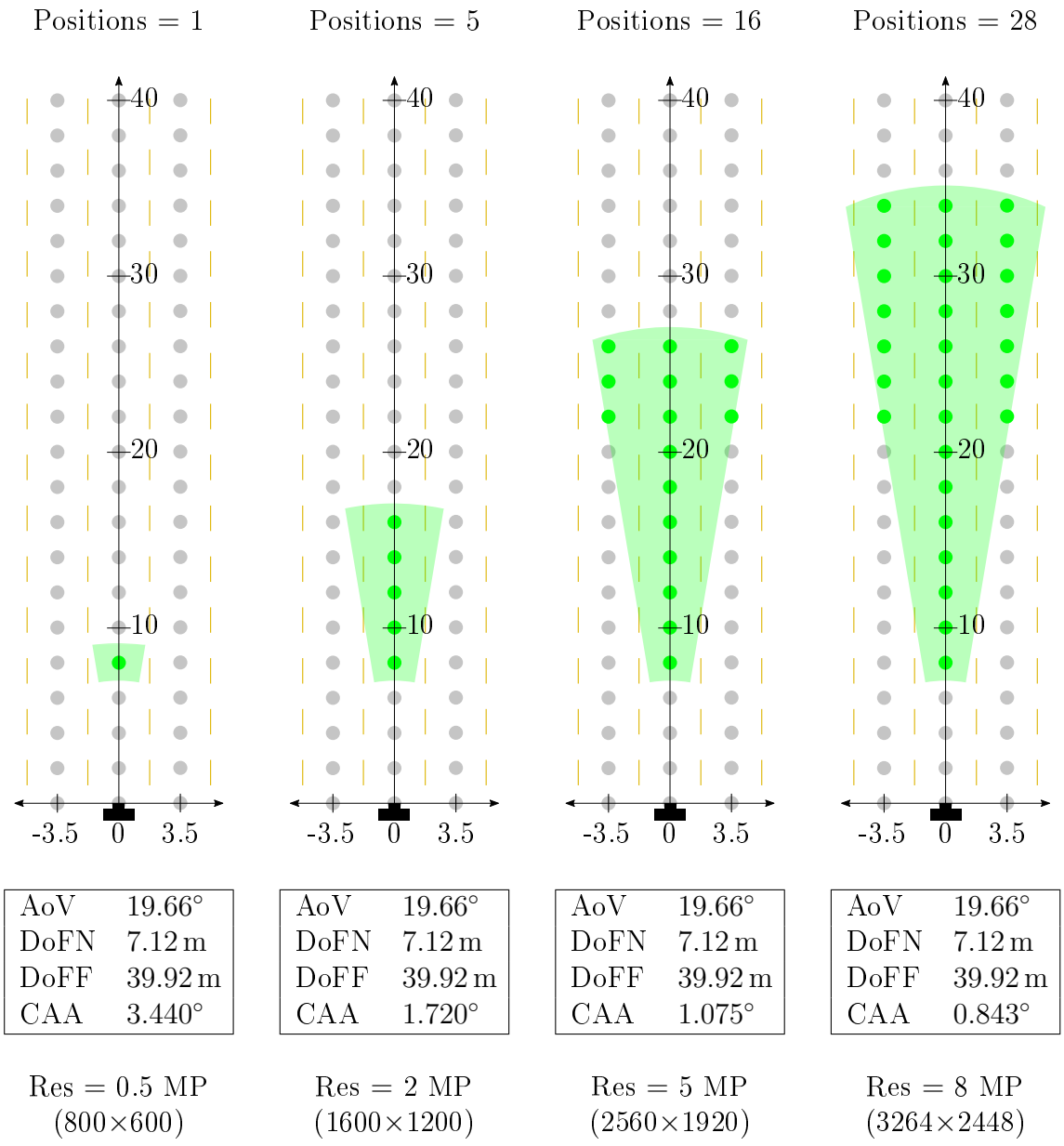

AoV	19.66°	AoV	19.66°	AoV	19.66°	AoV	19.66°
DoFN	7.12 m	DoFN	7.12 m	DoFN	7.12 m	DoFN	7.12 m
DoFF	39.92 m	DoFF	39.92 m	DoFF	39.92 m	DoFF	39.92 m
CAA	3.440°	CAA	1.720°	CAA	1.075°	CAA	0.843°
Res = 0.5 MP (800×600)		Res = 2 MP (1600×1200)		Res = 5 MP (2560×1920)		Res = 8 MP (3264×2448)	

Figure 3.15: Simulated GREs and derived properties for various sensor resolutions (axis in meters)

3.3.5 Image Sensor Size

A variation of sensor size affected all three derived properties and gave rise to an interesting phenomenon. An increasing sensor size slightly widened the AoV, shortened DoFN and increased both the DoFF and CAA, as shown in Figure 3.16.

It is noteworthy that the far recognition range fluctuated for increasing sensor size. This was due to both the DoFF and CAA increasing, creating an effect comparable to that observed in the focal length analysis and illustrated in Figure 3.17. In this case, an increasing DoFF extended the far range for sensor types 1/3.6", 1/3.2" and 1/3.0", while the increasing CAA shortened far range at larger sensor sizes. This relationship produced the rise and fall of far range seen in the simulated GREs.

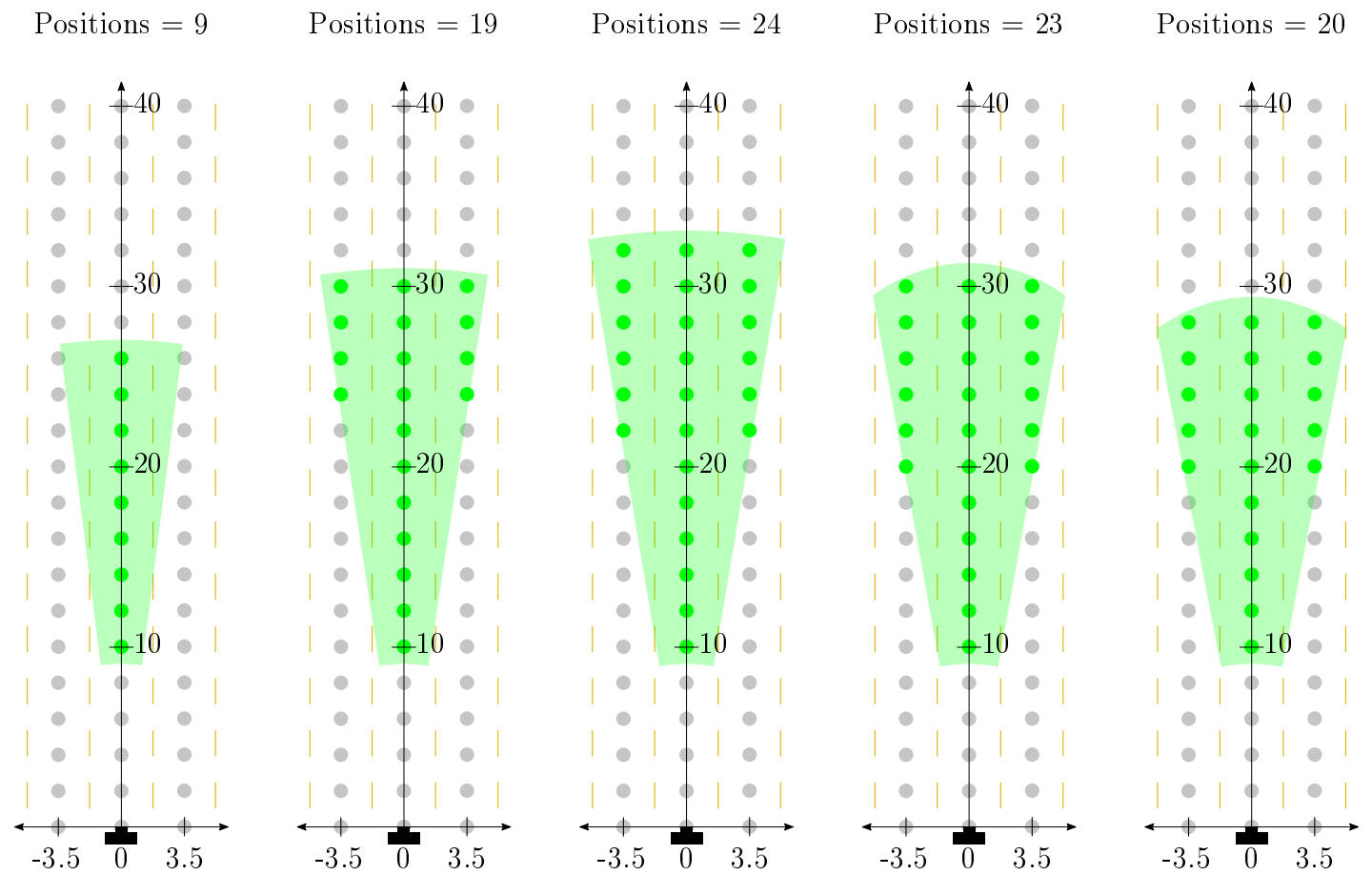

AoV	16.26°	AoV	18.28°	AoV	19.46°	AoV	21.58°	AoV	23.25°
DoFN	9.49 m	DoFN	9.12 m	DoFN	8.92 m	DoFN	8.57 m	DoFN	8.31 m
DoFF	26.77 m	DoFF	30.23 m	DoFF	32.72 m	DoFF	38.44 m	DoFF	44.62 m
CAA	0.697°	CAA	0.784°	CAA	0.834°	CAA	0.926°	CAA	0.997°
Type = 1/3.6"		Type = 1/3.2"		Type = 1/3.0"		Type = 1/2.7"		Type = 1/2.5"	

Figure 3.16: Simulated GREs and derived properties for various sensor types (axis in meters)

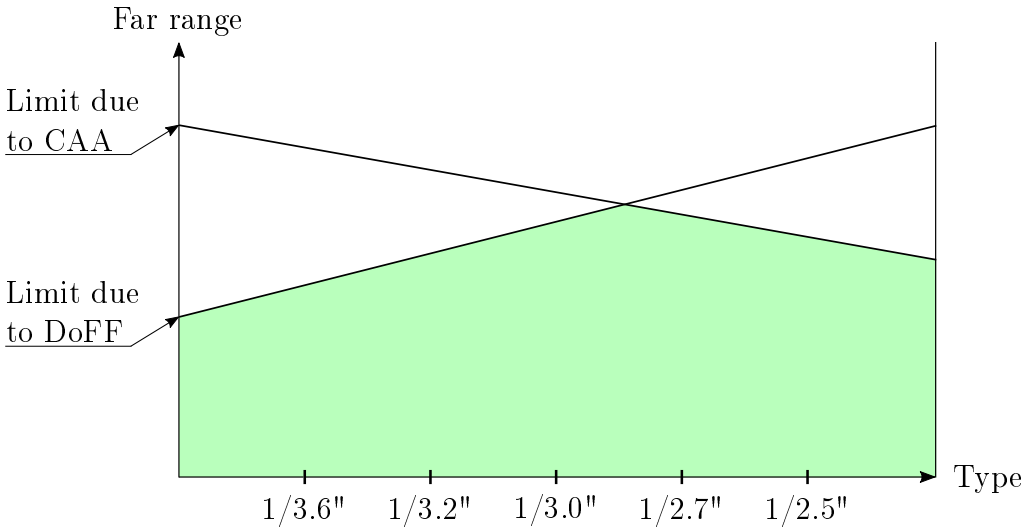

Figure 3.17: The relationship between CAA and DoFF as far range limiting factors for various sensor sizes. The shaded region represents the GRE and is determined by the nearest limiting factor.

3.4 Experimental Results Discussion and Model Validation

Initially, a large discrepancy existed between the empirically measured recognition areas and the corresponding simulated GREs. This was considered to be possibly due to the inaccuracy of the lens adjustment rings, even when set to their extreme settings.

To verify the actual focal lengths used in the experiment, the AoV was measured from the captured photos and substituted into the AoV equation (Equation 3.1) together with the image sensor width. From this, the actual focal lengths were calculated as 2.61 mm and 9.15 mm, significantly different from the 2.8 mm and 12 mm claimed to be the limits of the camera.

Furthermore, the unmarked adjustment rings made it impossible to determine the exact lens extension used in the two experimental camera configurations. Consequently, lens extension values were selected to produced GREs that resembled the measured recognition areas as closely as possible. The GREs were simulated using the updated primary properties shown in Table 3.4.

Property	Value
Focal length	2.61 mm, 9.15 mm
Lens extension	4 µm, 10 µm
Aperture	f/1.8
Sensor resolution	3264x2448 (8MP)
Sensor size	1/3.2" (5.7mm diagonal)

Table 3.4: Primary camera properties used for the experiment and model validation

3.4.1 Short Focal Length Configuration

The short focal length configuration produced a recognition area almost identical to the simulated GRE, as shown in Figure 3.18. An in-depth analysis into the cause of recognition failure at the edge of the recognition area provided greater insight into the minute differences between the two regions.

The far range of both regions were limited by licence plate resolution. In the simulation this is evident from the GRE not being limited by the DoFF, implying the CAA as the limiting factor. In the case of the experiment, this was determined by cropping out the furthest recognisable licence plate.

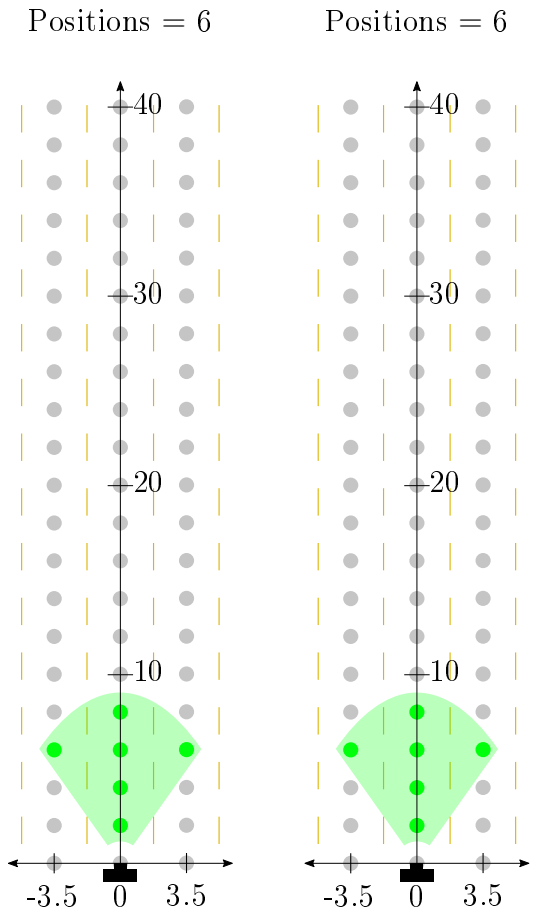

(a) Experimental (b) Simulated

Figure 3.18: Experimentally measured recognition area and simulated GRE comparison for the short focal length camera configuration (axis in meters)

The cropped licence plate is shown in Figure 3.19. The successful recognition is indicated by a green tick, while recognition failure will be shown by the presence of a red cross. The cropped licence plate was reasonably focused, but comprised only 135×28 pixels. This is a mere 3.6% less than the 140 horizontal pixels used as the theoretical recognition requirement, evidence that insufficient resolution limited the far range of the recognition area.

(a) Captured photo (9 m) (b) Cropped licence plate (133×27 pixels)

Figure 3.19: Furthest experimentally recognisable licence plate with short focal length camera configuration

According to the simulation, the near recognition range was determined by the DoFN. However, photos taken of near licence plates, shown in Figure 3.20, displayed no sign of being out of focus.

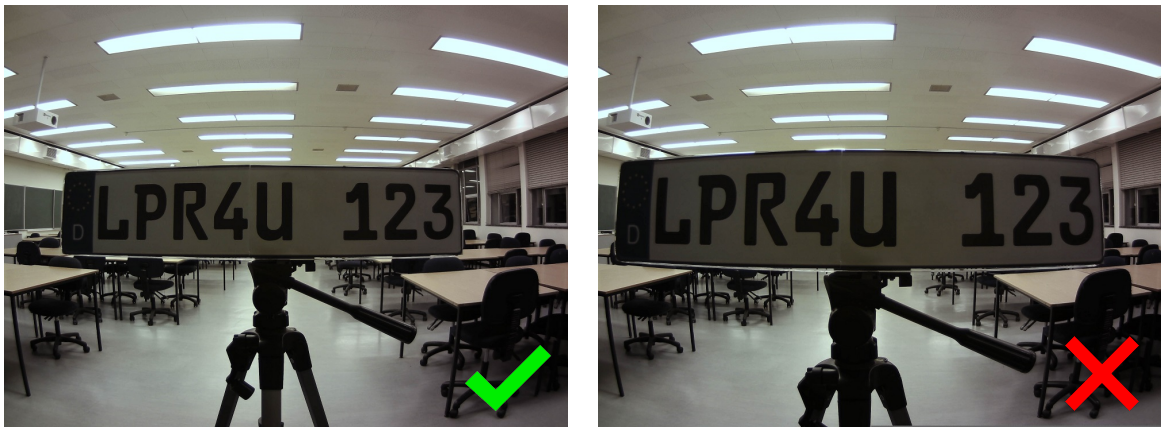

(a) 0.5 m (b) 0.4 m

Figure 3.20: Nearest experimentally recognisable licence plate with short focal length camera configuration

The actual reason for recognition failure was determined by applying various image correction techniques to a licence plate located just outside of the recognition area. The techniques required to make the licence plate recognisable would identify the original cause of recognition failure. In the case of Figure 3.20b, successful recognition was

achieved after the application of brightness and pincushion correction, as shown in Figure 3.21.

(a) Brightening correction applied. Recognition still failed.

(b) Brightening and pincushion correction applied. Recognition successful.

Figure 3.21: Successful recognition of Figure 3.20b after application of correction techniques

Use of these techniques identified insufficient lighting and barrel distortion as the near range limiter of the experimentally measured recognition area. Neither of these factors were incorporated in the theoretical model.

The insufficient lighting was therefore attributed to the edge of the test range being poorly lit. Although omitted from the theoretical model, the effect of lighting was thoroughly examined in the analysis of environmental factors and is included in Chapter 4.

On the other hand, barrel distortion occurs in cameras with large AoVs. It effects the entire image and is evidenced by the curved ceiling lights in Figures 3.19 and 3.20. The amount of curvature is greater for objects far away from the center of the frame (such as the ceiling lights), with limited curvature occurring at the frame center. Because of this, the edges of a licence plate approaching the camera would at some point reach critical curvature at which recognition would fail.

It should be noted that given the experimental AoV used, barrel distortion only hindered recognition at a range of 0.4 m or less. This is shorter than the bonnet (hood) of most vehicles and as such would not limit the effective near recognition capability of a dashboard-mounted camera.

It is also noteworthy that a licence much closer than 0.4 m would not be recognised due to it exceeding the AoV and not being wholly visible within the frame, regardless of lighting conditions and optical distortion. This confirms that focus was in no way responsible for limiting the near range of the experimentally measured recognition area. Instead, bar lighting conditions and optical distortion, a near licence could be recognised up until the point where its width exceeded the AoV.

3.4.2 Long Focal Length Configuration

The long focal length configuration produced a recognition area similar to the simulated GRE, barring a noticeable difference in same-lane coverage, as shown in Figure 3.22. Once again, the reasons for recognition failure at the extremities of the recognition area was investigated to gain deeper insight into the differences observed between the two regions. It is noteworthy that both regions feature identical coverage of adjacent lanes, validating the use of AoV in modelling the width of the recognition area.

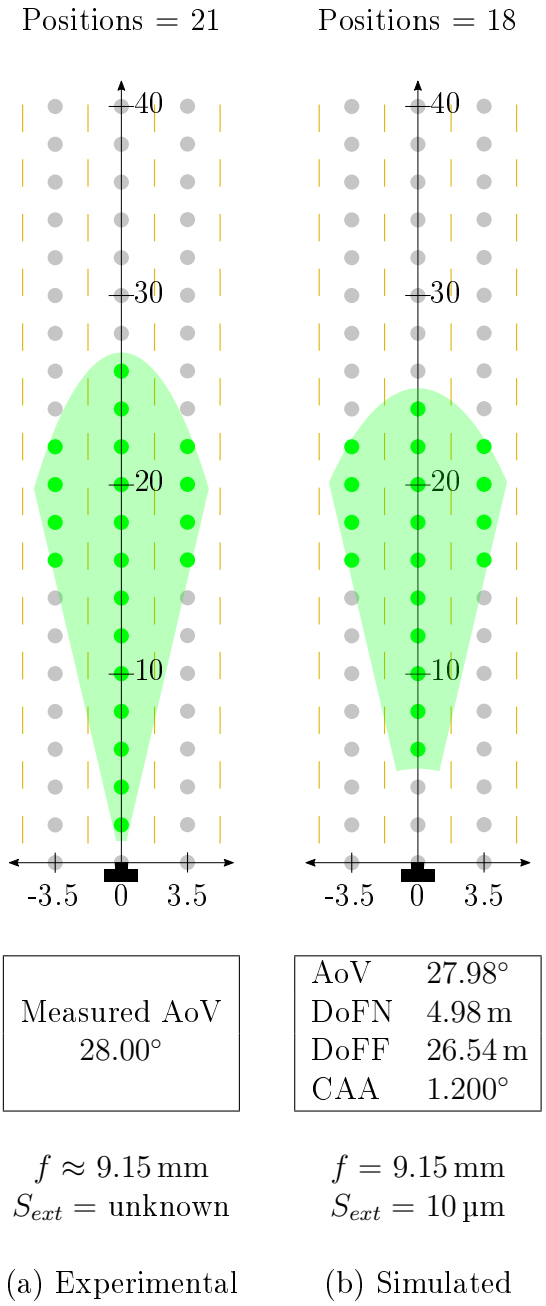

Figure 3.22: Experimentally measured recognition area and simulated GRE comparison for the long focal length camera configuration (axis in meters)

In both the experiment and simulation, far range was again limited by licence plate resolution. In the simulation, this is apparent by die GRE not being limited by the

DoFF, but instead by the CAA. The furtherest experimentally recognisable licence plate was cropped and measured, as shown in Figure 3.23. The cropped licence plate consisted of only 120×25 pixels, 14% less than required in the theoretical model. This difference explained the shorter range of the simulated GRE.

(a) Captured photo (27 m) (b) Cropped licence plate (120×25 pixels)

Figure 3.23: Furthest experimentally recognisable licence plate with long focal length camera configuration

The simulated near recognition range was limited by DoFN. However, photographs of near licence plates were well in-focus, but dark, as shown in Figure 3.24.

(a) 2 m (b) 1 m

Figure 3.24: Nearest experimentally recognisable licence plate with long focal length camera configuration

By applying brightening correction, near licence plates previously unrecognisable could be recognised, as demonstrated in Figure 3.25. This established insufficient lighting as the near range limit of the experientially measured recognition area. As in the short focal length configuration, a licence plate any closer than 1 m would exceed the AoV and therefore not be recognised, regardless of lighting conditions. This attested to focus not limiting the near range of the recognition area. Instead, given sufficient lighting conditions, a near licence could be recognised as long as it remains wholly within the AoV.

Figure 3.25: Successful recognition of Figure 3.24b after brightening correction

3.5 Summary

Increasing the camera focal length narrowed the AoV and CAA while extending the DoF further away from the camera, producing a long and narrow GRE with greater overall size when projected onto the road surface. This resulted in near licence plates in adjacent lanes no longer being visible, but far licence plate being captured in sufficient focus and resolution for accurate recognition. The experiment confirmed this result and showed the theoretical model to be accurate.

Increasing of the lens extension resulted in a small and near DoF, effectively shrinking the GRE size when projected onto the road surface. Although this brought near licence plates within focus, it also resulted in far licence plates becoming out of focus. A large recognition area could potentially be achieved using an appropriate fixed-focus lens.

Decreasing of aperture size, as realized by the use of a larger f-number, shortened the DoFN and extended the DoFF, thereby expanding the GRE in both the near and far directions. This resulted in a greater area being captured in sufficient focus for recognition, especially at far range.

The use of higher resolution image sensors significantly decreased the CAA, thereby extending the far GRE boundary. This allowed licence plates to be capture in sufficient resolution at much greater range.

Finally, a greater sensor size slightly widened the AoV and CAA, shortened the DoFN and extended the DoFF. This produce a wider GRE with slight variance in far range. Licence plates in adjacent lanes were only recognisable when using medium to large sensors.

Although each of these primary properties affected the GRE shape, some were more influential than others. Focal length and lens extension afforded great flexibility in manipulating the GRE shape, especially regarding coverage of adjacent lanes and far range. Similarly, a high-resolution sensor allowed licence plates to be recognised at a range otherwise unachievable. In comparison, aperture and sensor size exhibited a relatively small effect on the GRE.

Chapter 4

Environmental Factors

After completion of the optoelectronic analysis, the focus of this work shifted to consider the impact of environmental factors on recognition accuracy. These factors are external to the camera and exist within the system's operational environment. As such, environmental factors affect recognition accuracy independently of camera properties. This work specifically focused on the effect of relative motion and orientation between licence plates and camera, as well as lighting conditions.

Experiments were designed to capture the distortion commonly caused by these three factors. The type and amount of distortion created would effectively limit recognition accuracy to certain environmental conditions. In some cases, the distortion was measured and corrected using image manipulation techniques, thereby enhancing the recognition accuracy. Together, this provided an understanding into how individual environmental factors affect recognition accuracy.

4.1 Experimental Configuration

A specific experiment was designed for the analysis of each environmental factor. This approach was chosen due to the difficulty involved in accurately simulating the real-world distortions produced by environmental factors. In each experiment, the licence plate was positioned well within the recognition area and care was taken to minimise distortion caused by other environmental factors. This allowed for any limitation of recognition accuracy to be ascribed to the factor under investigation.

4.1.1 Relative Motion

Relative motion between the licence plate and camera occurs constantly in urban driving. The effect of relative motion on recognition accuracy was analysed by separating the motion into two orthogonal components and conducting a subsequent experiment.

4.1.1.1 Components of Relative Motion

Relative licence plate motion was separated along two orthogonal axes: Motion towards or away from the camera was referred to as longitudinal motion, while motion that maintained the distance between the licence plate and camera was termed lateral motion, as shown in Figure 4.1. This figure utilises the perspective projection model discussed in Section 3.1.3.3 on page 22.

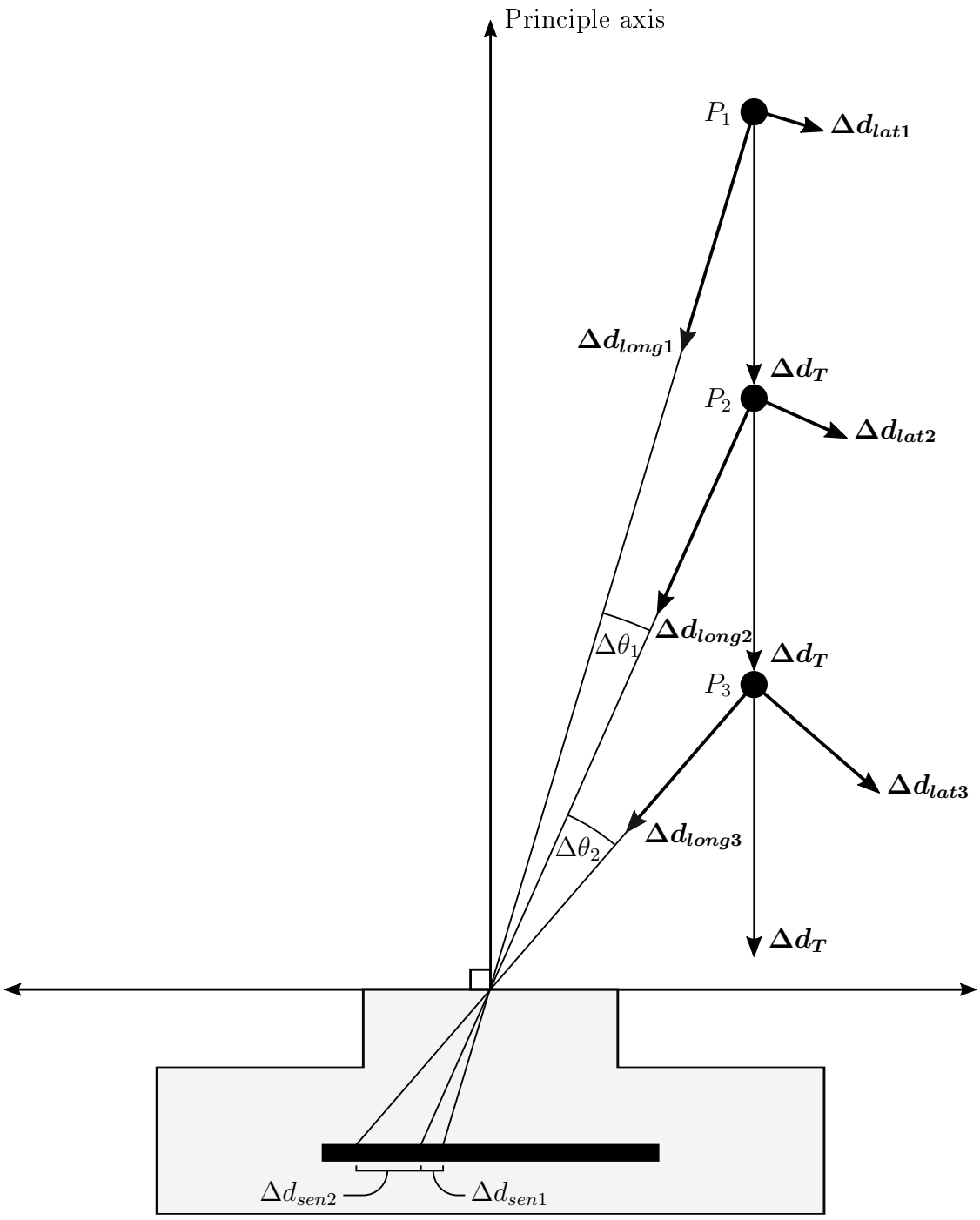

$P_{[n]}$	Object position
$\boldsymbol{\Delta d_T}$	Travel vector
$\boldsymbol{\Delta d_{long[n]}}$	Longitudinal motion component
$\boldsymbol{\Delta d_{lat[n]}}$	Lateral motion component
$\Delta\theta_{[n]}$	Angle rotated around camera
$\Delta d_{sen[n]}$	Distance moved on sensor

Figure 4.1: An object travelling with constant velocity relative to the camera's principle axis exhibits both longitudinal and lateral motion. The amount of lateral motion corresponds to the distance moved by incoming light on the image sensor and consequently, the amount of motion blur.

The figure illustrates an object travelling with constant velocity relative to the camera's principle axis, displayed at three positions with equal time and distance intervals. The travel vector consists of a longitudinal and lateral component. The lateral component relates to the angle rotated around the camera. This angle corresponds to the distance moved by light from the object on the image sensor.

Given the equal time interval between positions, greater lateral motion would relate to a larger distance moved on the image sensor. This would relate to a greater amount of motion blur for a given effective exposure time. From this, it was concluded that the lateral component of relative motion contributes to the phenomenon of motion blur.

This relationship is clearly demonstrated in Figure 4.2. The streetlamps near the edge of the image experienced a relatively large amount of lateral motion during effective exposure and consequently exhibit a great amount of motion blur. On the other hand, streetlamps near the center of the image experienced minimal lateral motion during effective exposure and are only slightly blurred.

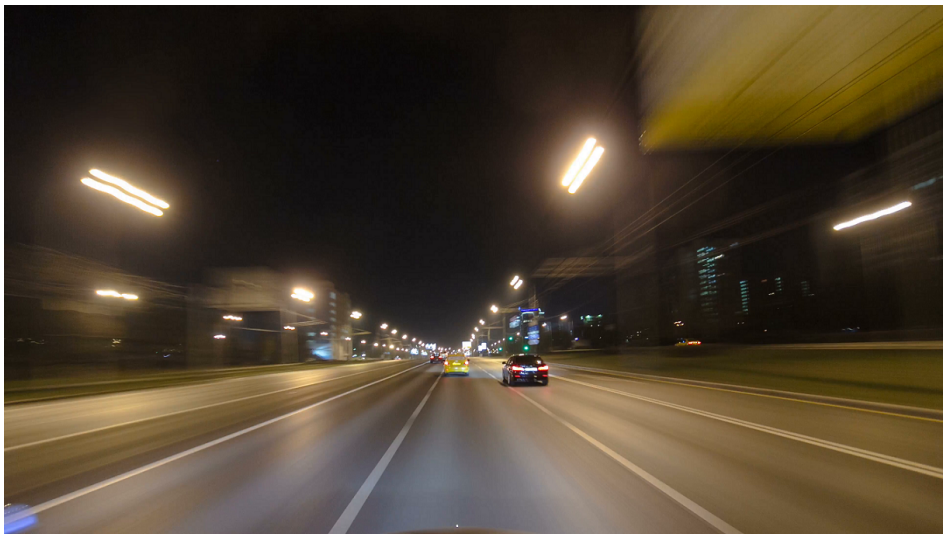

Figure 4.2: Typical example of motion blur in low light conditions. The streetlamps near the edge of the image demonstrate how objects with greater lateral motion produce a large amount of motion blur. [35]

Furthermore, lateral motion also described the licence plate movement producing slant distortion in rolling shutters cameras.

4.1.1.2 Lateral Motion Experiment

A lateral motion experiment requires strict control over the relative rotation of the licence plate around the camera. This was achieved by use of a single-axis rate table. Such an apparatus rotates a platform at a precise angular velocity and is commonly used for the testing of inertial systems. The camera system, including the Raspberry Pi and a battery pack, was mounted on the rate table, as shown in Figure 4.3. A licence plate, mounted on a static tripod, was positioned 5m away from the apparatus.

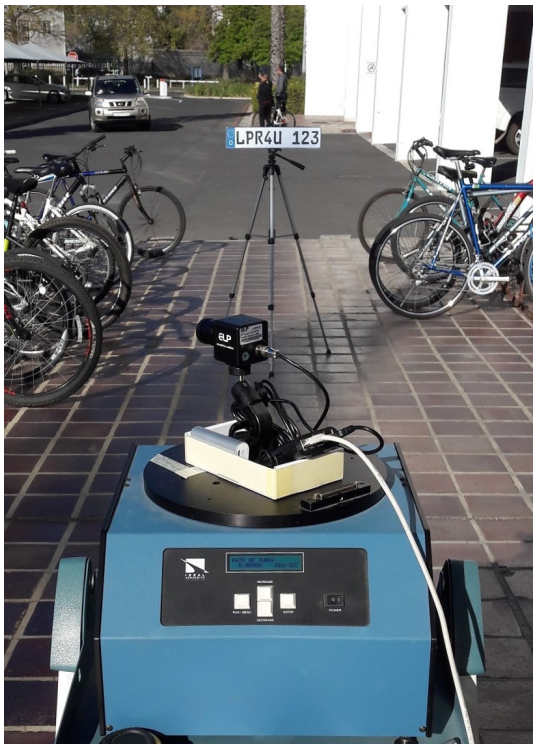

Figure 4.3: Lateral motion experiment configuration displaying the static licence plate as well as the experimental camera, Raspberry Pi and battery mounted on the rate table.

Rotating the entire camera system clockwise at different angular velocities accomplished the relative licence plate rotation required. The effect of lateral motion on recognition accuracy could be observed by capturing photographs at the instant the camera was aimed towards the licence plate.

Lighting is another important consideration in motion analysis. This is due to the mutual contribution of relative motion and light intensity towards the phenomenon of motion blur. The effect of lighting was incorporated by repeating the lateral motion experiment in two different lighting conditions. The light intensity of these conditions were significantly different, albeit not precisely measured. This approach would produced two sets of results from which the effect of both motion and lighting could be observed.

The lateral motion experiment was firstly conducted with bright afternoon sunlight shining directly onto the face of the licence plate. This was followed by an in-door experiment under dim florescent lighting, a condition similar to that produced by streetlamps.

4.1.2 Relative Orientation

The effect of relative orientation on recognition accuracy becomes apparent when a licence plate is not facing directly towards the camera. Such orientation results in perspective distortion which impairs recognition accuracy. The licence plate can be rotated away from the camera on the yaw, pitch and roll axes.

4.1.2.1 Yaw Rotation Experiment

Relative rotation on the yaw axis occurs repeatedly in urban traffic. Common examples include vehicles in adjacent lanes, those parked perpendicular to the road or any vehicle turned away from the camera. An experiment was designed to determine the effect of yaw rotation on recognition accuracy.

The experiment was conducted in a large in-door venue, allowing constant ideal lighting conditions. The camera and licence plate were once again mounted on static tripods to avoid the effect of relative motion being captured. The licence plate was positioned 5 m in front of camera and well within the GRE. The licence plate was progressively rotated and captured at increments of 11.25° ($\frac{1}{32}$ of a full rotation).

4.1.2.2 Pitch and Roll Discussion

Licence plates are rarely rotated on the pitch and roll axes. Significant pitch distortion may occur when a vehicle is positioned on a steep incline or a great height difference exists between the dashboard-mounted camera and a licence plate. Roll distortion can impair recognition when vehicles are located on uneven terrain, such as one side of the vehicle parked over a curb. Such conditions occur less frequently than those producing yaw distortion. As such, the effect of relative orientation on recognition accuracy was evaluated only in terms of rotation on the yaw axis.

4.1.3 Lighting Conditions

Various light sources may illuminate licence plates in urban traffic. The effect on recognition accuracy will depend on the direction, intensity and spectrum of such light. Bright sunlight and moderate artificial light were already evaluated as part of the lateral motion experiment. Another commonly occurring condition is that of night-time driving. This condition features the use of directional light from vehicle headlights and allows the retroflective property of licence plates to come to the forefront.

4.1.3.1 Night-time Test Environment

An experiment was designed to establish the effect of vehicle headlights and retroflective licence plates on recognition accuracy. This involved setting up a pitch dark test environment in a large in-door venue. Two high-power incandescent lamps were positioned either side of the camera, reproducing the typical configuration of headlights and a dashboard-mounted camera.

Both the camera and licence plate were mounted on static tripods to ensure that relative motion would not affect the experiment results. The camera was zoomed in and set to the maximum aperture opening. This would allow for results to be comparable to the recognition area of the long focal length camera configuration, which was measured in ideal lighting conditions.

4.1.3.2 Licence Plates Used

Due to the locale of this research, a retroflective EU licence plate was not readily available. Instead, a retroflective South African (SA) licence plate was sourced, shown in Figure 4.4.

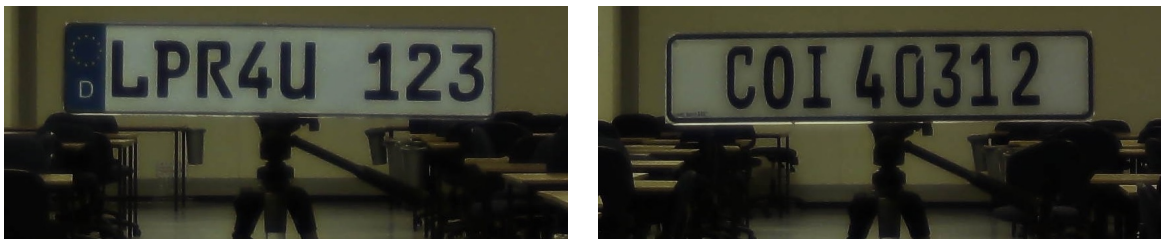

(a) Non-retroflective EU licence plate (b) Retroflective SA licence plate

Figure 4.4: Licence plates used for the night-time experiment

Unfortunately, the recognition algorithm did not included a SA licence plate classifier. This introduced an undesired mismatch between the format of the licence plate and that of the recognition algorithm, something that would inevitably impair recognition accuracy. However, both licence plates featured clear black characters on a white background and exhibited other similar characteristic. The mismatch of format would be taken into consideration when interpreting the experiment results.

Both the EU and SA licence plates were used in the night-time experiment and illuminated by lamps. The results would provide greater insight into the effectiveness of retroflection in aiding night-time recognition.

4.1.3.3 Oncoming headlights

Oncoming headlights can potentially cause lens flare and glare. This is problematic, due to the close proximity of a vehicle's headlights and licence plate. Lens effects may obscure the licence plate, rendering accurate recognition impossible. This phenomenon was investigated by capturing images of real-world oncoming traffic at night.

4.2 Results Discussion

Results of the lateral motion, yaw rotation and lighting experiments offered great insight into how these factors influence recognition accuracy. Some of the effects observed include slant, motion blur, yaw distortion and lens effects. Each of these effects limited the environmental conditions in which accurate recognition was possible.

4.2.1 Lateral Motion Experiment

The effect of relative lateral motion on recognition accuracy was grouped into the two distortions observed, namely slant and motion blur. Slant distortion occurred due to the use of a progressive scan shutter in the experimental camera and is related to the image sensor resolution and readout speed. Motion blur was captured due to the movement of incoming light during effective exposure and relates to the photosensor integration time.

4.2.1.1 Slant Distortion

The two lighting conditions used experienced an identical amount of slant for any given angular velocity, due to the constant sensor resolution and readout speed. However, the bright light experiment was primarily used for the evaluation of slant distortion due to its absence of motion blur. This allowed the amount of slant in degrees (ϕ) to be precisely measured from the sharp edges of licence plate characters. Furthermore, by avoiding motion blur, any limitation in recognition accuracy could be attributed to slant distortion. Twenty different angular velocities ($\dot{\theta}$) were evaluated, a selection of which is shown in Figure 4.5. Accurate recognition was achieved up to an angular velocity of 9°/s and approximately 13° of slant.

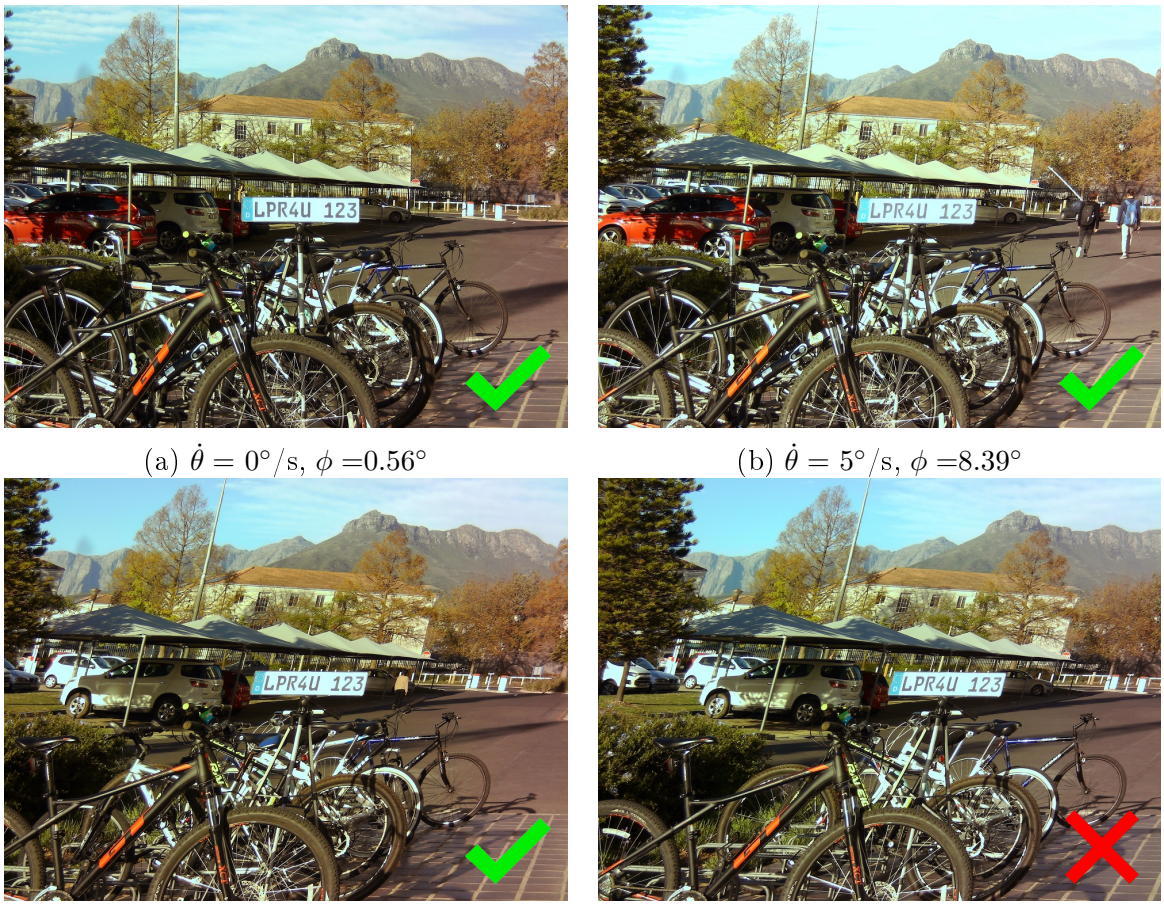

(a) $\dot{\theta} = 0°/s$, ϕ =0.56°

(b) $\dot{\theta} = 5°/s$, ϕ =8.39°

(c) $\dot{\theta} = 9°/s$, ϕ =12.96°

(d) $\dot{\theta} = 10°/s$, ϕ =14.75°

Figure 4.5: Licence plate captured in bright lighting conditions and at various angular velocities exhibiting slant distortion. Successful recognition was achieved for an angular velocity up to 9°/s.

Slant Correction

A slant correction algorithm was used to effectively counteract the effect of slant. Applying an appropriate amount of inverse slant enabled the recognition of licence plates otherwise unrecognisable. A demonstration is shown in Figure 4.6. The algorithm ran on a Raspberry Pi and executed within 0.26 seconds on average, irrespective of the amount of slant correction applied. Theoretically, such a technique can counteract any amount of slant, provided that the licence plate is still captured in sufficient resolution.

(a) $\dot{\theta} = 12°/\text{s}$, ϕ =16.79°

(b) The same image recognised after application of slant correction

Figure 4.6: Successful recognition is possible at greater angular velocities when slant correction is applied.

Effect of slant during turn manoeuvres

Considerable lateral motion typically occurs when a vehicle-mounted camera is turning through an intersection. Such movement generates slant which can limit recognition accuracy for the full duration of the turn. This, coupled with the frequency of turn manoeuvres in urban driving, motivated further analysis into the effect of slant on recognition accuracy in turn manoeuvres.

Such an evaluation required an understanding of how turn manoeuvres generate slant. An example of a common turn manoeuvre is shown in Figure 4.7. The angular velocity of the camera is dependent on its velocity (v) and the turn radius (r), as shown in Equation (4.1).

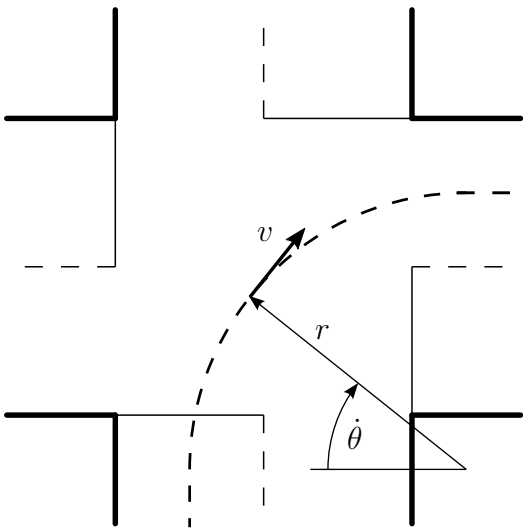

Figure 4.7: Illustration of a right turn through a 4-way stop displaying the camera velocity (v), camera angular velocity ($\dot{\theta}$) and turn radius (r).

$$\dot{\theta} = \frac{180v}{r\pi} \tag{4.1}$$

The amount of slant generated could be calculated from the angular velocity. This was possible due to measurements taken from the captured images. The relationship between angular velocity and slant was discovered to be proportional with a factor of approximately 1.325, as shown in Equation (4.2). This factor will be dependent on the resolution and readout speed of the specific image sensor used.

$$\phi \approx 1.325\dot{\theta} \tag{4.2}$$

Combining these two equations into Equation (4.3) provided a solution for the approximate amount of slant distortion generated in an arbitrary turn manouvre.

$$\phi \approx 238.5\frac{v}{r\pi} \tag{4.3}$$

This equation was plotted for four different degrees of slant, shown in Figure 4.8.

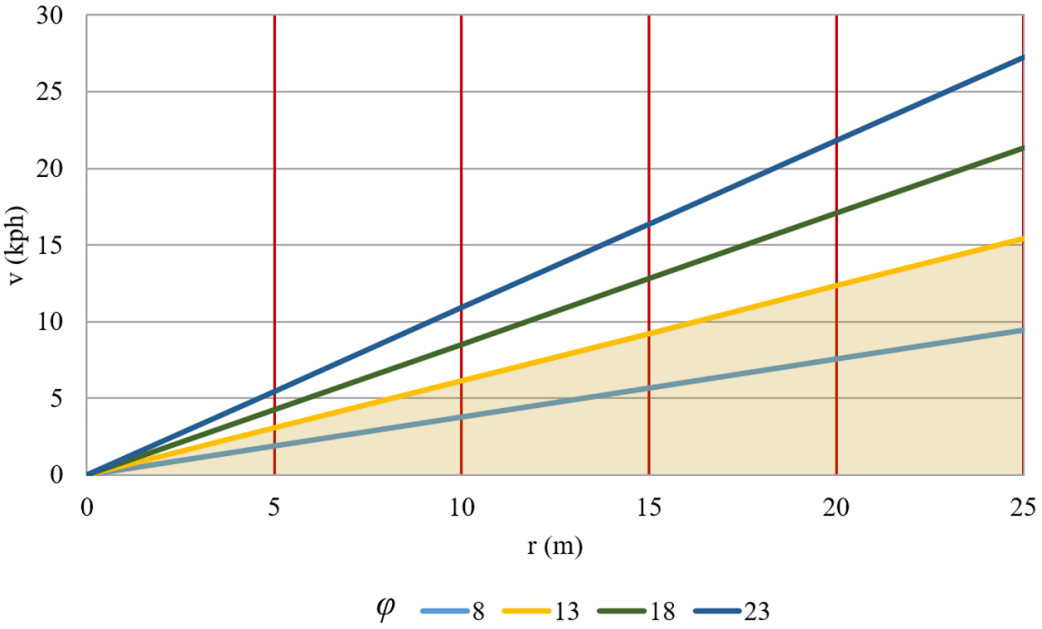

Figure 4.8: Four different degrees of slant produced as a result of camera velocity and turn radius.

The shaded region represents velocity and turn radius combinations which produce less than 13° of slant. The experimental camera could theoretically execute such turn manoeuvres in bright lighting conditions without impairing recognition accuracy. The application of slant correction would enable the recognition of licence plates with even greater slant. This would effectively extend the recognition capability, allowing accurate recognition in manoeuvres with greater velocity and tighter turn radiuses.

To relate this model to real-world traffic scenarios, the turn radiuses of four types of urban intersections were measured and is shown in Table 4.1. It should be noted that these turn radiuses apply to a road network in which vehicles drive on the left side.

Type of intersection	Turn direction	r(m)
Small circle	Right	6
All	Left	10
4-Way stop	Right	15
Signalised	Right	20

Table 4.1: Typical vehicle turn radiuses of various intersection types

Figure 4.8 could be interpreted using these values to provide the maximum vehicle velocity in km/h at which specific turns could be executed in bright lighting conditions without impairing recognition accuracy. For example, the experimental camera can accurately recognised licence plates while making a left turn at 6 km/h or while making a right turn through a signalised intersection at 12 km/h. The use of slant correction to recognise licence plates with up 23° of slant increases these velocities to 11 km/h and 22 km/h, respectively.

4.2.1.2 Motion Blur

The prevalence of motion blur differed significantly between the bright and moderate lighting condition. This was due to the integration time being automatically adjusted to achieve optimal exposure. Licence plates captured in bright lighting conditions revealed no noticeable evidence of motion blur. This remained the case even at high angular velocity, as shown in Figure 4.9. Such a licence plate could be accurately recognised after the application of slant correction, as demonstrated in the previous section. The absence of motion blur can be attributed to the abundance of ambient light in the scene. This resulted in a pixel integration time sufficiently short to avoid creation of noticeable motion blur.

Figure 4.9: Licence plate captured in bright lighting conditions at $\dot{\theta} = 12°/s$. No evidence of motion blur is noticeable

However, the moderate lighting experiment produced distinct evidence of motion blur, due the use of a slower integration time. Some of the licence plates captured are shown in Figure 4.10. Accurate recognition was only achieved up to an angular velocity of 1.5°/s. Past this point, character edges became too blurred to be accurately recognised, despite still being legible to the human eye. Characters started to overlap at an angular velocity of 2.5°/s and became indistinguishable at 6°/s.

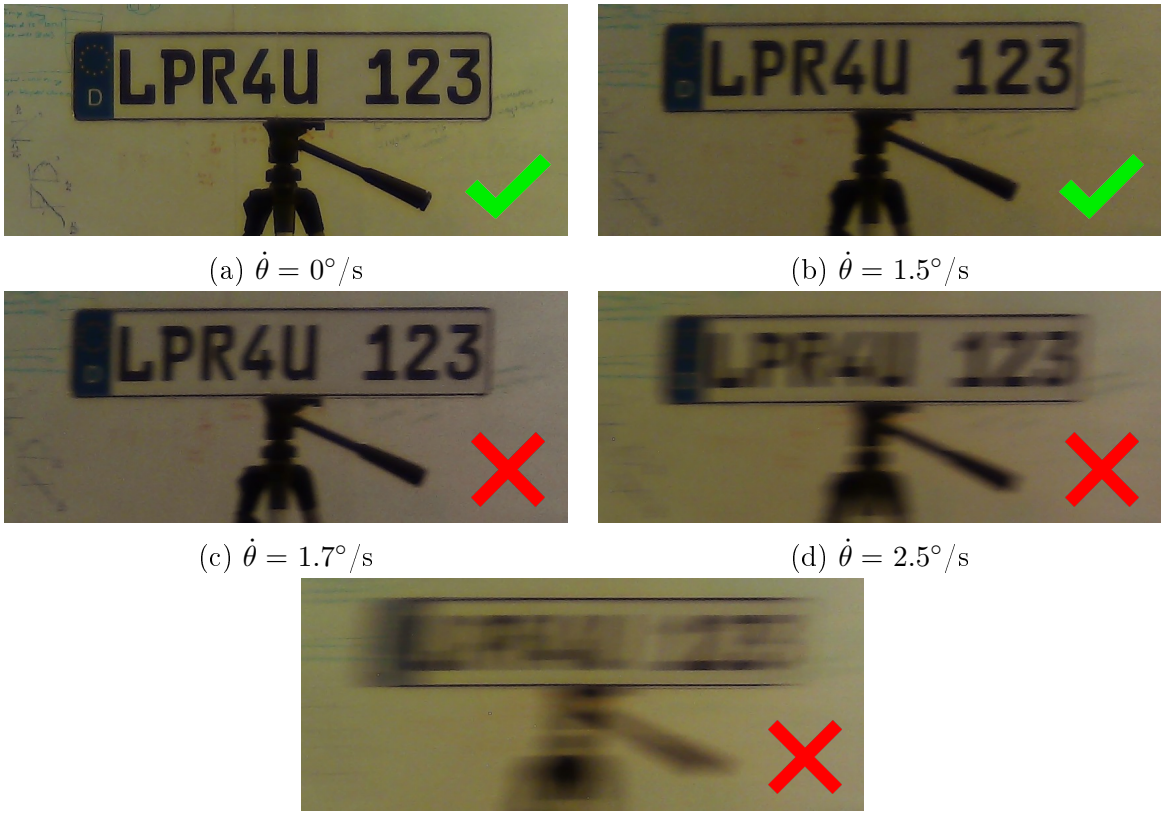

(a) $\dot{\theta} = 0°/s$ (b) $\dot{\theta} = 1.5°/s$

(c) $\dot{\theta} = 1.7°/s$ (d) $\dot{\theta} = 2.5°/s$

(e) $\dot{\theta} = 6°/s$

Figure 4.10: Licence plates with lateral motion captured in moderate lighting conditions. The effect of motion blur can be clearly seen and increases with greater angular velocity.

The contribution of poor lighting and lateral motion to the occurrence of motion blur were clearly observed. These experiments indicated that motion blur does not limit recognition accuracy in bright lighting conditions. In moderate lighting conditions, motion blur significantly impaired recognition accuracy, even at low angular velocity.

Equation (4.1) and Table 4.1 were used to calculate the maximum vehicle velocity in km/h at which specific turns could be executed in moderate lighting conditions while still accurately recognising licence plates. These values would offer insight into how motion blur limits recognition accuracy in typical traffic scenarios. Accurate recognition would theoretically be possible during a 0.9 km/h left-hand turn or a 1.8 km/h right-hand turn through a signalised intersection.

4.2.2 Yaw Rotation Experiment

The effect of yaw distortion was clearly evident in licence plates captured during the yaw rotation experiment. As shown in Figure 4.11, the amount of horizontal compression increased as the licence plate was rotated further away from the camera. Recognition failed when the licence plate was rotated past 45°.

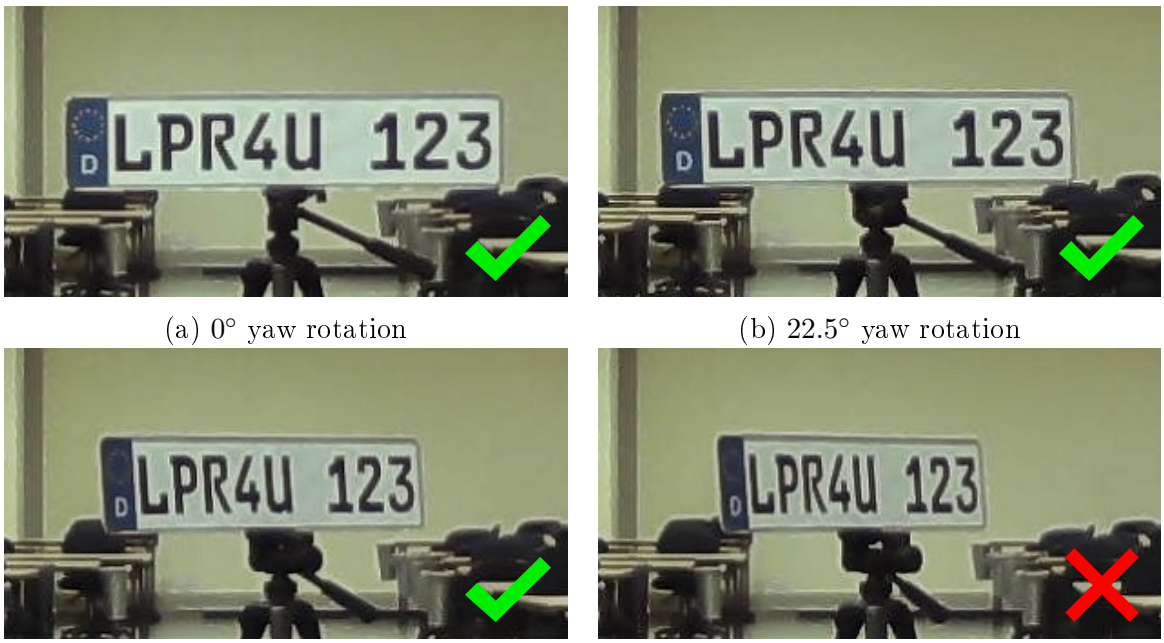

(a) 0° yaw rotation (b) 22.5° yaw rotation

(c) 45° yaw rotation (d) 56.25° yaw rotation

Figure 4.11: Licence plates with various degrees of yaw rotation. Successful recognition was achieved for yaw rotation up to 45°.

The recognition failure could either be due to the distorted licence plate shape or insufficient licence plate resolution. The latter was considered a possibility due to the lower resolution of the rotated licence plate.

A experiment was conducted to determine the true cause of recognition failure. The distance between the licence plate and camera was shortened to only 2 m and the camera zoomed in. This produced an image with high licence plate resolution. Still, successful recognition was only achieved for yaw rotation up to 45°, as shown in Figure 4.12. This ruled out insufficient resolution as the cause of recognition failure. Instead, perspective distortion hindered the recognition of licence plates past 45° of yaw rotation. This surpassed the 15° limitation of some commercial systems [33].

(a) 45° yaw rotation (b) 56.25° yaw rotation

Figure 4.12: Recognition of high-resolution licence plates still fail past 45° of yaw rotation.

4.2.2.1 Stretch Correction

Yaw rotation distorted licence plates into a trapezoid shape. This effect was most notable using near licence plates and a zoomed-in camera, as demonstrated in Figure 4.12. Such distortion can be corrected using planar homography. However, the vertical distortion component became negligible for licence plates further than 2 m away. As such, the effect of yaw rotation could be approximated to horizontal compression. This type of distortion can be remedied by stretching the image until the licence plate reaches its original aspect ratio. An example of this is shown in Figure 4.13.

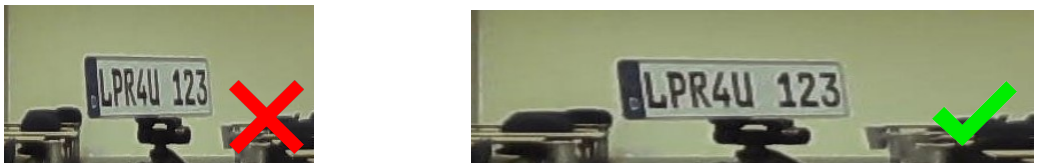

(a) 67.50° yaw rotation (b) Stretch correction applied. Recognised.

Figure 4.13: A licence plate with 67.50° yaw rotation. Successful recognition was achieved after the application of stretch correction.

The captured image was stretched by multiplying its width by a scale factor. The appropriate scale factor depended on the amount of yaw distortion in the original image. Theoretically, stretch correction could be used to remedy the effect of arbitrarily large yaw rotation, provided that the licence plate was still captured in sufficient resolution. The stretch correction was preformed on a Raspberry Pi and the execution time in seconds (t_{strech}) was dependant on the scale factor (SF), as shown in Equation (4.4).

$$t_{strech} = 0.88SF - 0.455 \tag{4.4}$$

4.2.2.2 Explanation of Unwanted Slant

The tripod mount used in experimentation required that the licence plate be tilted back slightly. This minimal setting did not affect any of the other experiments but did introduce unwanted slant in the yaw rotation experiment. Such slant is visible in Figures 4.11 and 4.13. However, Figure 4.13 also demonstrates that slant did not hinder the successful recognition achieved by the use of stretch correction. Figure 4.14 demonstrates the same process with slant removed. Once again, successful recognition is achieved after the application of stretch correction.

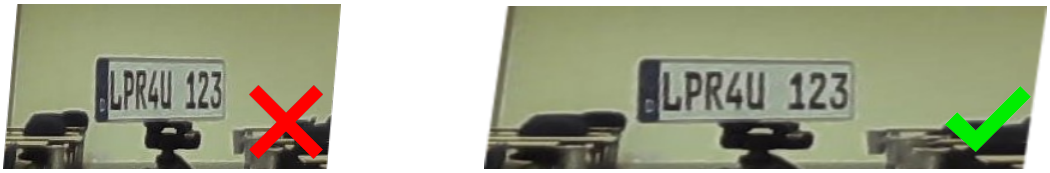

(a) Slant removed. Recognition still failed. (b) Stretch correction applied. Recognised.

Figure 4.14: Unwanted slant produced by the experimental setup was removed. Once again, successful recognition was only achieved after the application of stretch correction.

4.2.3 Night Driving Experiment

Images captured during night-time lighting conditions provided insight into how vehicle headlights and retroflective licence plates influence recognition accuracy. The tremendous effectiveness of retroflection in night-time recognition became apparent, as well as the ability of oncoming headlights to impair recognition.

4.2.3.1 Retroflection

The non-retroflective EU licence could be accurately recognised up to a range of 5 m, as shown in Figure 4.15. However, it is worth noting that only a single character was misidentified at 10 m, even though the licence plate was practically indistinguishable to the human eye (Past this point, recognition utterly failed). This is due to the remarkable ability of the algorithm to detect edges and effectively recognise licence plates of the same format as its classifier.

(a) 5 m (b) 10 m

Figure 4.15: A non-retroflective EU licence plate illuminated by lamps and captured at various distances. At 10 m only a single character was misidentified, despite the image appearing simply black to the human eye.

The retroflective SA licence plate could be reasonably recognised up to a range of 20 m, as shown in Figure 4.16.

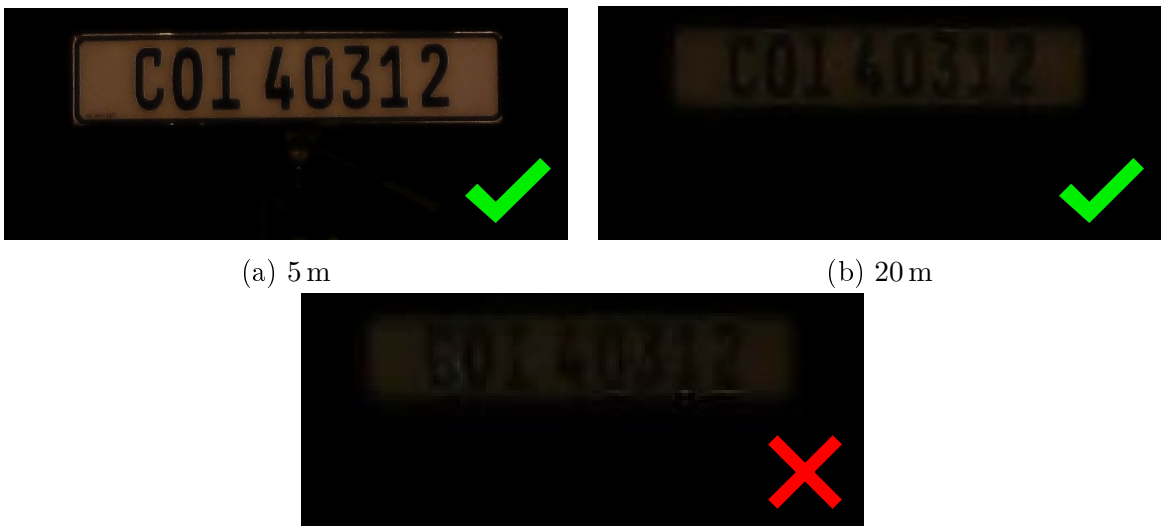

(a) 5 m (b) 20 m

(c) 25 m

Figure 4.16: A retroflective SA licence plate illuminated by lamps and captured at various distances. Recognition was reasonably accurate up to a range of 20 m.

An allowance of two characters being misidentified was included to compensate for the mismatch of the SA licence plate with an EU format classifier. Given the near-accurate recognition of the non-retroflective EU licence plate at 10 m, the use of a retroflective licence plate approximately doubled the recognition range. It is expected that a EU format retroflective licence plate would match, or perhaps even out perform, the 27 m range achieved in ideal lighting conditions in Chapter 3.

4.2.3.2 Lens Effects

Lens flare and glare readily occurred in images of oncoming vehicles during night-time. The size and extent of these artefacts varied depending on the angle between the vehicle and camera. When sufficiently large, lens flare and glare obstructed the licence plate and made recognition impossible, as shown in Figure 4.17. Lens flare was present mainly along a specific section of the vehicle's approach, while glare remained as long as the headlights were within the frame.

Figure 4.17: Example of lens flare and glare obscuring the licence plate of an oncoming vehicle during night-time driving.

4.3 Summary

In moderate lighting conditions, lateral motion limited recognition accuracy due to motion blur. In bright lighting conditions, a greater amount of lateral motion was tolerable before recognition accuracy was impaired due to slant distortion. Slant correction was demonstrated to effectively enhanced recognition accuracy in bright lighting conditions.

Furthermore, perspective distortion limited the relative orientation between camera and licence plate to less that 45° of yaw rotation for accurate recognition to be possible. Licence plates with a greater amount of yaw rotation could be accurately recognised using a stretch correction technique.

Finally, retroflection was shown to effectively double the range of night-time recognition while oncoming headlights were prone to produced lens effects that were problematic to recognition.

Chapter 5

Conclusion

The chapter contains a review of the two primary research objectives, followed by a summary, discussion of possible future work and closing remarks.

5.1 Evaluation of Objectives

This work set out to determine how, and to what degree, optoelectronic and environmental factors affect the overall ability of vehicle-mounted licence plate recognition (LPR) systems to correctly identify licence plates. This task was separated into two primary research objectives.

5.1.1 Effect of Optoelectronic Factors

The effect of optoelectronic factors on recognition accuracy was specifically analysed in terms of the region in which the system could correctly identify licence plates. This was referred to as the recognition area. The effect of individual primary camera properties on the recognition area was investigated using a theoretical model and an experiment.

5.1.1.1 Theoretical Model

A model was developed which classified licence plates as recognisable based on known photographic criteria of accurate recognition. This criteria was subsequently redefined in terms of derived camera properties. From this, the geometric recognition envelope (GRE) was defined to model the recognition area.

Next, a theoretical framework was formulated by which the GRE could be determined for any given focal length, lens extension, aperture size, sensor resolution and sensor size. The model was implement as a simulation and effectively calculated the GREs of multiple typical compact camera configurations. The results exhibited clear trends in the effect of individual primary camera properties on recognition area.

Focal length greatly determined far recognition range, as well as coverage of adjacent lanes. Use of a manual focus, or appropriate fixed-focus lens was demonstrated to be sufficient for achieving a large recognition area. Furthermore, a great recognition range was achieved using a high-resolution image sensor of any physical size. Finally, although aperture size affected recognition area, it would also affect low-light recogni-

tion accuracy and should rather be selected based on the lighting conditions in which the camera will typically operate.

5.1.1.2 Model Validation

The model was validated using results from a representative experiment. The recognition area of two different camera configurations were empirically measured using an actual camera and recognition algorithm. The GREs of the same camera configurations were also simulated. The measured recognition areas and simulated GREs were remarkably similar, varying only slightly in the case of the long focal length configuration. The experiment also exhibited a similar trend in how a change of focal length effected recognition area. The model was concluded to be an effective tool for estimating the effect of individual camera properties on recognition area.

5.1.2 Effect of Environmental Factors

The work considered the effect of motion, orientation and lighting on recognition accuracy. The effect of each factor was experimentally identified and quantified.

5.1.2.1 Motion

Lateral motion of licence plates relative to the camera was proven to be the primary cause of slant distortion and motion blur. Such motion was discovered to limit recognition accuracy due to slant distortion when turning at more than 9°/s in bright lighting conditions. In moderate lighting conditions, lateral motion limited recognition accuracy due to motion blur when turning at more than 1.5°/s. The maximum velocity in km/h was determined at which a vehicle-based camera could execute various turn manoeuvres while still accurately recognising licence plates. The use of slant correction effectively extended recognition accuracy to include turn rates of up to 12°/s in bright lighting conditions.

5.1.2.2 Orientation

Rotation on the yaw axis was motivated to be the most common variance in orientation between vehicles in urban traffic. Subsequently, 45° of relative yaw rotation between camera and licence plate was proven to limit recognition accuracy. The use of stretch correction enable the accurate recognition of licence plates with up to 67.50° of relative yaw rotation.

5.1.2.3 Lighting

Low lighting conditions were shown to significantly increase the amount of motion blur in the captured image. In night-time conditions, a retroflective licence plate could be recognised at approximately double the range of a non-retroflective licence plate. However, oncoming headlights produced lens effects which impaired accurate recognition.

5.2 Summary

This work successfully showed how different optoelectronic and environmental factors significantly affect the recognition accuracy of vehicle-mounted LPR systems.

Optoelectronic factors greatly determine the region in which licence plates can be accurately recognised. Although the shape of this region can largely be manipulated using a variable-focus zoom lens, it is possible to achieve a significant recognition area using an appropriate fixed-focus prime lens. Additional funds should rather be used to invest in a high-resolution image sensor, enabling the recognition of licence plates at a much greater distance, although also introducing a greater susceptibility to slant distortion during lateral motion.

Furthermore, recognition accuracy is impaired in certain environmental conditions. These include execution of turn manoeuvres, licence plates orientated at an angle to the camera and oncoming night-time traffic. Nevertheless, the range of night-time recognition approximates that achieved in daylight due to the retroflective characteristic of licence plates. Recognition accuracy can also be enhanced to include a greater variation of environmental conditions using image correction techniques, such as slant and stretch correction.

Such insight will aid in the selection of an appropriate camera for use in low-cost open source LPR systems and provide a realistic understanding of the limitations of recognition accuracy in various environmental and traffic conditions.

5.3 Future Work

This section elaborates on remaining challenges related to this work, as well as recommendations and possible future research.

5.3.1 Remaining Challenges

This work could not experimentally establish the effect of focus on recognition accuracy. Although the effect of the depth of field was clearly demonstrated in the theoretical model, factors other than focus impaired recognition accuracy in the experimental test. Further tests may be conducted to experimentally determine how insufficient focus may limit recognition accuracy. From this, a circle of confusion factor may be empirically calculated that describes the recognition algorithm's robustness to unfocused licence plates.

The mutual effect of optoelectronic and environmental factors was not considered. This included the relationship between environmental lighting conditions and camera exposure settings, such as aperture size and effective exposure time. Similarly, the combined effect of angle of view and relative motion was excluded from this investigation. Analysis of such factor combinations may provide a more comprehensive understanding of recognition accuracy in different conditions.

5.3.2 Recommendations

A theoretical optoelectronic model can be an accurate and cost-effective tool for selecting an appropriate camera for a desired recognition area. Also, the use of a large indoor test environment greatly aids in the precise control of environmental conditions, and provides reliable and repeatable results.

Where possible, the properties of a new camera should be inspected and validated as claims made in datasheet may not be entirely accurate. This was the case with the experimental camera's zoom lens, which offered a third less focal length range than claimed.

5.3.3 Subsequent Research

This work prepares the way for research into various other aspects of LPR technology. An investigation into operational factors such as camera vibration, mounting position and traffic patterns may add an entire new dimension to the understanding of an LPR system's capability. Evaluation of processing factors such as hardware component choice, automated image correction and algorithm optimisation may also offer useful insight.

Finally, a multi-agent network of low-cost open source vehicle-mounted LPR systems is considered a very attractive solution for use in developing countries, one which will require extensive further research drawing on expertise from many knowledge fields.

5.4 Closing Remarks

This work provided great insight into the complex working of digital cameras. The multitude of interdependent optoelectronic factors was initially overwhelming, but was eventually worked into an effective model based on an understanding of the fundamentals. Testing of environmental factors also proved to be an insightful journey, especially when observing the effect of real-world traffic behaviour on the performance of electronic systems, such as LPR.

In hind sight, greater emphasis would have been on analysing recognition accuracy in actual driving conditions. This would have demonstrated a complete test of the experimental system and allowed other influential factors to be identified.

Appendix A

Constant Primary Properties used in Optoelectronic Model

The theoretical analysis of individual primary camera properties required that other primary properties be kept constant. These tables detail the constant properties used for each analysis.

Property	Value
Lens extension	12 µm
Aperture	f/2.4
Sensor resolution	3264x2448 (8MP)
Sensor size	1/3.2"

Table A.1: Constant primary properties used for focal length analysis

Property	Value
Focal length	15.5 mm
Aperture	f/2.0
Sensor resolution	3264x2448 (8MP)
Sensor size	1/3.2"

Table A.2: Constant primary properties used for lens extension analysis

Property	Value
Focal length	14 mm
Lens extension	16 µm
Sensor resolution	3264x2448 (8MP)
Sensor size	1/3.2"

Table A.3: Constant primary properties used for aperture size analysis

Property	Value
Focal length	13 mm
Lens extension	14 µm
Aperture	f/2.6
Sensor size	1/3.2"

Table A.4: Constant primary properties used for sensor resolution analysis

Property	Value
Focal length	14 mm
Lens extension	14 µm
Aperture	f/2.0
Sensor resolution	3264x2448 (8MP)

Table A.5: Constant primary properties used for sensor size analysis

List of References

[1] "Crime Stats SA." [Online]. Available: http://www.crimestatssa.com/national.php

[2] Police Executive Research Forum, *How Are Innovations in Technology Transforming Policing?*, 2012. [Online]. Available: https://web.archive.org/web/20130129220334/http://policeforum.org/library/critical-issues-in-policing-series/Technology_web2.pdf

[3] M. Hoctor, "Mass surveillance system nicks drivers," 2012. [Online]. Available: https://www.illawarramercury.com.au/story/113726/mass-surveillance-system-nicks-drivers/

[4] K. Deb, A. Vavilin, and K. H. Jo, "An efficient method for correcting vehicle license plate tilt," in *Proceedings - 2010 IEEE International Conference on Granular Computing, GrC 2010*, 2010, pp. 127–132. [Online]. Available: http://ieeexplore.ieee.org/document/5576175/

[5] P. Hurtik and M. Vajgl, "Automatic license plate recognition in difficult conditions - Technical report," in *IFSA-SCIS 2017 - Joint 17th World Congress of International Fuzzy Systems Association and 9th International Conference on Soft Computing and Intelligent Systems*, 2017, pp. 0–5. [Online]. Available: http://ieeexplore.ieee.org/document/8023337/

[6] C. T. Nguyen, T. B. Nguyen, and S. T. Chung, "Reliable detection and skew correction method of license plate for PTZ camera-based license plate recognition system," in *International Conference on ICT Convergence 2015: Innovations Toward the IoT, 5G, and Smart Media Era, ICTC 2015*, 2015, pp. 1013–1018. [Online]. Available: http://ieeexplore.ieee.org/document/7354726/

[7] D. Bailey, D. Irecki, B. Lim, and L. Yang, "Test bed for number plate recognition applications," in *Proceedings First IEEE International Workshop on Electronic Design, Test and Applications '2002*, 2002, pp. 0–2. [Online]. Available: http://seat.massey.ac.nz/research/centres/SPRG/pdfs/2002_DELTA_501.pdf

[8] P. Chhoriya, G. Paliwal, and P. Badhan, "Image Processing Based Automatic Toll Booth in Indian Conditions," *International Journal of Emerging Technology and Advanced Engineering*, vol. 3, no. 4, pp. 410–414, 2013. [Online]. Available: https://pdfs.semanticscholar.org/c553/c0b3abf7e4abc69a3d7e711bed58c80fa39d.pdf

[9] L. W. Chen, Y. C. Tseng, and K. Z. Syue, "Surveillance on-the-road: Vehicular tracking and reporting by V2V communications," *Computer Networks*, vol. 67, pp. 154–163, 2014. [Online]. Available: http://dx.doi.org/10.1016/j.comnet.2014.03.031

[10] "AutoVu | Genetec." [Online]. Available: https://www.genetec.com/solutions/all-products/autovu

[11] HTS, "HTS Vehicle Recognition Solutions VRS M100 IMAGING UNIT," Tech. Rep., 2015. [Online]. Available: http://x.htsol.com/wp-content/uploads/2015/06/HTS-Mobile-Enforcement.pdf

[12] ——, "HTS Vehicle Recognition Solutions VRS DR200 IMAGING UNIT," Tech. Rep., 2014. [Online]. Available: http://x.htsol.com/wp-content/uploads/2014/11/DR-200.pdf

[13] "ELSAG: Leader In Fixed & Mobile ALPR Systems." [Online]. Available: https://www.elsag.com/

[14] "PIPS Technology - Detection Innovation." [Online]. Available: http://www.pipstechnology.com/

[15] "OpenALPR - Automatic License Plate Recognition." [Online]. Available: http://www.openalpr.com/

[16] "JavaANPR - Automatic number plate recognition system." [Online]. Available: http://javaanpr.sourceforge.net/

[17] M. Sarfraz, M. Ahmed, and S. Ghazi, "Saudi Arabian license plate recognition system," in *2003 International Conference on Geometric Modeling and Graphics, 2003. Proceedings*, 2003, pp. 36–41. [Online]. Available: http://ieeexplore.ieee.org/document/1219663/

[18] L. Liu, S. Zhang, Y. Zhang, and X. Ye, "Slant Correction of Vehicle License Plate Image," in *International Conference on Image Analysis and Processing*, vol. 3617, 2005, pp. 237–244. [Online]. Available: https://link.springer.com/content/pdf/10.1007%2F11553595_29.pdf

[19] P. S. Ha and M. Shakeri, "License Plate Automatic Recognition based on edge detection," in *Artificial Intelligence and Robotics (IRANOPEN)*. IEEE, 2016, pp. 170–174. [Online]. Available: http://ieeexplore.ieee.org/abstract/document/7529509

[20] D. Malacara and Z. Malacara, *Handbook of Optical Design*, 2nd ed. New York: Marcel Dekker, Inc, 2004. [Online]. Available: http://optdesign.narod.ru/book/Handbook_of_Optical_Design.pdf

[21] HTS, "HTS Vehicle Recognition Solutions VRS N60L IMAGING UNIT," Tech. Rep., 2015. [Online]. Available: http://x.htsol.com/wp-content/uploads/2015/11/N60L.pdf

[22] D. Hart, *The Camera Assistant: A Complete Professional Handbook*. Focal Press, 1996. [Online]. Available: https://books.google.co.za/books?id=HjwrBgAAQBAJ

[23] L. Bortner, "Lens Equation," University of Cincinnati Department of Physics, Tech. Rep., 2013. [Online]. Available: http://homepages.uc.edu/~bortnelj/labs/Physics3experiments/LensEquation/LensEquationhtm.htm

[24] H. Zimmermann, *Silicon Optoelectronic Integrated Circuits*. Springer, 2004. [Online]. Available: https://books.google.co.za/books?id=VmJJObEuIj4C

[25] Qimaging, "Rolling Shutter vs. Global Shutter," Tech. Rep., 2014. [Online]. Available: https://www.qimaging.com/ccdorscmos/pdfs/RollingvsGlobalShutter.pdf

[26] O. Yadid-Pecht and R. Etienne-Cummings, *CMOS Imagers: From Phototransduction to Image Processing*. Kluwer Academic Publishers, 2004. [Online]. Available: https://books.google.co.za/books?id=5dQRBwAAQBAJ

[27] J. Nakamura, *Image Sensors and Signal Processing for Digital Still Cameras*. Taylor & Francis, 2005. [Online]. Available: https://books.google.co.za/books?id=UY6QzgzgieYC

[28] R. Bassom and G. Rixon, "INS-DAS-29: Operations manual for UltraDAS," Isaac Newton Group of Telescopes, Tech. Rep., 2011. [Online]. Available: http://www.ing.iac.es/~docs/ins/das/ins-das-29/integration.html

[29] B. Peterson, *Understanding exposure: How to shoot great photographs with any camera*, 4th ed. Berkeley: Amphoto Books, 2016. [Online]. Available: https://books.google.co.za/books?id=vCDzCQAAQBAJ

[30] ——, *Understanding shutter speed: Creative action and low-light photography beyond 1/125 second*. Amphoto Books, 2008. [Online]. Available: https://books.google.co.za/books?id=lVFDduFmMf4C

[31] N. L. Salvaggio, *Basic Photographic Materials and Processes*, L. D. Stroebel and R. D. Zakia, Eds. Focal Press, 2009. [Online]. Available: https://books.google.co.za/books?id=71uE_OrGw5oC

[32] B. A. Barsky, "Depth of Field and Hyperfocal Distance Equations and Approximations," UC Berkeley College of Engineering, Tech. Rep., 2005. [Online]. Available: http://inst.eecs.berkeley.edu/~cs39j/sp05/handouts/depth.of.field.writeup.html

[33] GeoVision Inc., "Troubleshooting LPR Issues," Tech. Rep., 2014. [Online]. Available: http://pd.geovision.tw/faq/AccessControl/LPR_Troubleshoot.pdf

[34] S. Du, M. Ibrahim, M. Shehata, and W. Badawy, "Automatic license plate recognition (ALPR): A state-of-the-art review," *IEEE Transactions on Circuits and Systems for Video Technology*, vol. 23, no. 2, pp. 311–325, 2013. [Online]. Available: http://ieeexplore.ieee.org/document/6213519/

[35] User Masuzi, "Best Frame Rate For Time Lapse Driving | Framesite.co," 2018. [Online]. Available: https://framesite.co/best-frame-rate-for-time-lapse-driving/

[36] R. E. Fischer, B. Tadic-Galeb, and P. R. Yoder, *Optical system design*, 2, Ed. McGraw-Hill, 2008. [Online]. Available: https://books.google.co.za/books?id=c9mYJhG1VHgC&dq

[37] Zeiss, "Camera Lens News No . 1," Carl Zeiss' Camera Lens Division, Tech. Rep. 1, 1997.

[38] J. Kannala and S. Brandt, "A Generic Camera Model and Calibration Method for Conventional ,," in *IEEE Transactions on Pattern Analysis and Machine Intelligence*, vol. 28, no. 8, 2006, pp. 1335–1340. [Online]. Available: https://ieeexplore.ieee.org/document/1642666